universität wien

MASTERARBEIT / MASTER'S THESIS

Titel der Masterarbeit / Title of the Master's Thesis

„Characterization of murine prostate organoids as a preclinical model for prostate cancer“

verfasst von / submitted by

Zlata Pavlovicova, BSc

angestrebter akademischer Grad / in partial fulfilment of the requirements for the degree of

Master of Science (MSc)

Wien, 2020 / Vienna, 2020

Studienkennzahl lt. Studienblatt / degree programme code as it appears on the student record sheet:	A 066 877
Studienrichtung lt. Studienblatt / degree programme as it appears on the student record sheet:	Masterstudium Genetik und Entwicklungsbiologie
Betreut von / Supervisor:	Assoc. Prof. Dr. Gerda Egger

Table of Contents

Table of Figures

Table of Tables

1 Introduction

Noncommunicable diseases such as most cancers have become a major public health problem worldwide in the last decades and are now responsible for about 1 in 6 deaths globally (Stewart and Wild 2014). As prostate cancer (PCa) is the second most common malignancy in men (Bray et al. 2018), understanding its biology is fundamental for the development of new therapeutic strategies.

Although many prostate tumours present as indolent and non-aggressive disease, some tumours progress to metastatic cancer with limited therapeutic options (Culig 2014). In order to understand the biology driving the transformation to aggressive PCa, it is essential to develop suitable preclinical models.

PCa research has been dominated by 2D cell cultures, patient-derived xenografts and animal model systems as the basis of PCa related studies. Often, these models are not able to mimic the situation *in vivo* accurately considering for instance the lack of organ-specific functions or genetic tumour heterogeneity in 2D cell cultures. Mouse cancer models have also certain limitations. Even though there is a variety of different genetic engineering tools to generate inducible, transgenic mouse model systems and these systems have had a major impact on the knowledge of cancer that we possess today, they are often time consuming, expensive and require a high number of mice that must be sacrificed (Cunningham and You 2015).

In recent years, a new *in vitro* model system was successfully introduced (Lancaster and Knoblich 2014). The organoid technology has been one of the biggest scientific advancements of the last decade. Prostate-derived organoids represent a three-dimensional simplified version of the organ which can be generated from normal and malignant prostate tissue and allow us to study different aspects of prostate biology from basic biological functions to tumorigenesis (Drost et al. 2016). Not only this technology possesses several advantages over existing approaches, it also has potential to revolutionize biomedical research as such – for instance in improving personalized medicine, developing new drug therapies and of course cancer modelling (Xu et al. 2018).

However, maintenance of human prostate organoids has proven to be challenging and only PCa organoids of metastatic disease were published to be successfully established as long

term cultures so far. To the contrary, mouse organoids are readily established from normal prostate and primary tumours and thus represent a great alternative model system to study PCa (Drost et al. 2016). Mouse primary PCa organoids can be generated having different genetic backgrounds, which enables to study the effects of the disruption of a certain gene or combination of genes. For instance, *Pten* and *p53* are tumour suppressor genes, or anti-oncogenes, that are commonly mutated in PCa. Loss of those genes leads to disruptive cell signalling continuing onto cell proliferation and cancer progression (The Molecular Taxonomy of Primary Prostate Cancer 2015; Berger et al. 2011). Additionally, mouse prostate organoids derived from normal epithelia can be genetically modified to generate *in vitro* knockouts of PCa relevant genes and such *in vitro* knockout systems represent a new organoid model to analyze the processes of malignant transformation.

1.1 Project description

The aim of this project is to establish a panel of normal and malignant murine organoid cultures harboring different genetic knockouts of PCa relevant genes such as *Pten* and a combination of *Pten*/*Stat3* and *Pten*/*Tp53* genes. The organoids were derived from tumour tissue of transgenic mice of different genetic backgrounds and healthy prostates of wildtype Cre-negative mice with floxed alleles that served as a control. Also, tamoxifen inducible *in vitro* knockout of *Pten* and a double knockout of *Pten*/*Stat3* were generated from benign murine prostate organoids. The organoid cultures were further characterized via immunohistochemistry and compared to their tissue of origin regarding their morphology and signalling pathways.

In future applications, the murine prostate organoid system will serve as a test model for drug screens to further dissect oncogenic signalling and sensitivities in the context of different genetic deletions.

2 Prostate cancer (PCa)

2.1 Epidemiology

Cancer is the second leading cause of death globally. In 2018, 9.6 million deaths were estimated to be caused by cancer and its incidence and mortality are continuously

increasing given the population growth and aging. PCa is the most frequently diagnosed cancer among men in most countries in the world and second leading cause of cancer death in 46 countries. According to estimates of Global cancer statistics, about 1.3 million of new cases worldwide were diagnosed in 2018 and about 1/4 of those patients died due to PCa. On a global scale, Caribbean countries show the highest incidence of PCa followed by Australia/New Zealand, Northern and Western Europe and North America. Mortality rates differ to incidence rates except in Caribbean where both mortality and incidence of PCa dominate. High mortality rates are mainly seen in developing countries of Africa (Fig.1) (Bray et al. 2018).

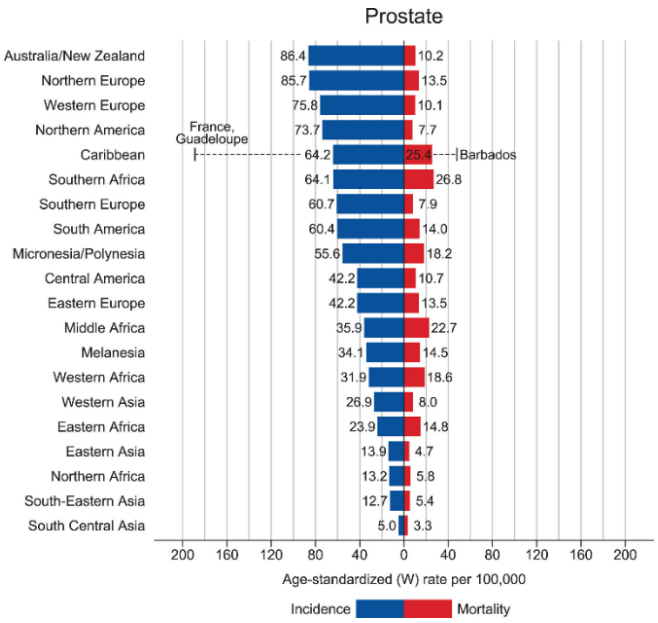

Figure 3
Bar Chart of incidence and mortality of PCa in 2018. The rates are world age-standardized and are shown in declining order (Bray et al. 2018).

2.2 Risk factors

The majority of cases (about 99%) of PCa occurs predominantly in older men above the age of 50. Apart from age, having a first-degree relative suffering from the disease increases the primary risk significantly. In the United States, the rates are the highest in men with African roots than in the White American population, which reflects the predisposition connected to the ethnic and genetic background. Additional risk factors may include a diet high in processed and red meat and low in vegetables of certain type (Stewart and Wild 2014).

2.3 Screening and diagnosis

The clinical behaviour of primary PCa highly varies – some men develop indolent cancer while others experience aggressive cancer leading to metastasis. As early PCa is usually asymptomatic, routine screening allows early detection and diagnosis. Screening for PCa takes place in form of measuring the recognized biomarker - prostate specific antigen (PSA) in sera (McGrath et al. 2016) usually in combination with digital rectal examination. PCa is eventually confirmed based on biopsy of the prostate tissue. Early diagnosis of PCa through screening allows early intervention prior to the disease progression, although PSA screening remains controversial regarding whether it improves therapy outcome. Evidence suggests that PSA-based screening leads to over diagnosis and over treatment of prostate tumours (Draisma et al. 2009).

2.4 Pathophysiology

The prostate is part of the male reproductive system. It is an exocrine gland that secretes and stores seminal fluid. It is located in the pelvis surrounded by the urethra, below the urinary bladder and in front of the rectum (Aumüller 1979). Growth and proper function of prostate cells depends on male hormones known as androgens. Androgens are required for the development of the normal prostate tissue but also play an important role in development of PCa (Taplin and Ho 2001). Prostate abnormalities may arise in the form of prostatic intraepithelial neoplasia (PIN), which further on leads to neoplastic transformation effecting the secretory epithelium lining, prostatic ducts and acini. PIN classifies in two grades – low-grade PIN and high-grade PIN (HG-PIN). Low-grade PIN causes cells to develop enlarged cell nuclei varying in size while all the nuclei in HG-PIN are of a similar large size. The cells effected by HG-PIN also possess increased chromatin content and prominent nucleoli that have a similar appearance to those of carcinoma cells. Evidence suggests that HG-PIN might be a precursor of prostate tumours (Montironi et al. 2007).

Most PCas are classified as adenocarcinomas, in which the epithelial tissue of glandular origin undergoes transformation into malignant tissue. Prostate adenocarcinomas are graded based on architectural features with the help of the Gleason grading system using samples from biopsy or surgery. The Gleason grading system is used to predict prognosis

and for therapy selection. Biopsy samples are microscopically examined and scored from 1-5 based on certain patterns such as resemblance to normal prostate tissue, the level of gland differentiation and presence of invading cells into surrounding tissue (Gleason and Mellinger 1974) as illustrated in Fig. 2. Higher Gleason scores correlate with more aggressive tumours and a worse prognosis (Humphrey et al. 2016). As the PCa progresses, prostate tumour cells may spread through the bloodstream or lymphatic system and thus cause metastasis. Prostatic carcinoma shows a tendency to evoke lymph node and bone metastasis. While lymp node metastasis is common in most cancer entities, PCa is unique in developing bone metastasis. The resulting bone tumours also have a tendency to be osteoblastic (bone forming) whereas the majority of bone metastasis of lung or kidney cancers are osteolytic (bone lysing) (Logothetis and Lin 2005).

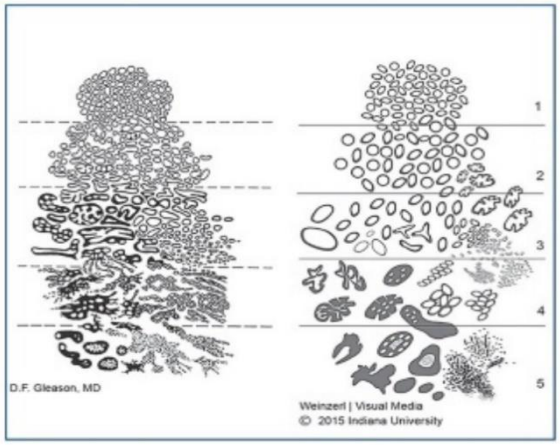

Figure 5
The original Gleason score system in comparison with the current state of Gleason grading (Sehn 2018).

2.5 Molecular pathology

PCa has been shown to be highly heterogeneous considering the clinical course of the disease as well as on a molecular level. The molecular pathology of PCa is complex, there is no single gene that is responsible for the development of PCa. Its pathogenesis is induced by genetic as well as environmental factors. Some of the molecular abnormalities of primary PCa have been identified and include DNA copy-number changes, gene rearrangements/fusions and mutations (Barbieri et al. 2012; Berger et al. 2011; Lapointe et al. 2007; Taylor et al. 2010). Because of those abnormalities, many genes and their downstream signalling pathways become effected and impaired. Among those genes are

cell cycle checkpoint genes, tumour suppressor genes, oncogenes and growth factors. For instance, the oncogene *c-MYC* was shown to be overexpressed in PCa and its overexpression is significantly correlated with the severity of the disease (Buttyan et al. 1987). Also mutations of the *CHEK2* gene, a regulator of the DNA damage signalling pathway, correlate with an increased risk of PCa (Cybulski et al. 2004). Numerous molecular changes in PCa also often alter androgen receptor (AR) and its downstream signalling. In fact, the most frequent molecular abnormality is the *TMPRSS2-ERG* gene fusion that is represented in about 50% of primary prostate tumours. *TMPRSS2* gene encodes a serine protease that is androgen regulated and its upregulation is linked to cancer cell growth (Tomlins et al. 2005). As a consequence of different molecular defects such as mutations/deletions/amplifications or structural changes of the AR itself, the AR signalling is often impaired and can result in androgen insensitivity (Brinkmann et al. 1991; Klocker et al. 1994). AR blockade is regularly used as a form of therapy to delay the progression of PCa. Tumour suppressor genes such as *Pten* and *p53* are frequently mutated in primary PCa and their loss or reduced expression plays an important role in the disease development and/or its progression (Wang and Wong 1997).

2.6 PCa relevant genes

2.6.1 ***PTEN***

PTEN (Phosphatase and tensin homolog) is localised on chromosome 10 in humans and acts as a tumour suppressor gene. Mutations/loss of *PTEN* were identified in many cancers and it was shown to be the most commonly lost tumour suppressor gene in primary PCa (The Molecular Taxonomy of Primary Prostate Cancer 2015; Berger et al. 2011). About 20% of primary prostate tumour samples at time of radical prostatectomy and about 50% of castration-resistant tumours show inactivation of *PTEN* by deletion or mutation (Jamaspishvili et al. 2018). Nevertheless, the rate of *PTEN* deletion in PCa varies depending on the type of study and the assay used to determine *PTEN* status. For instance several surgical cohorts using fluorescence in situ hybridization (FISH) identified *PTEN* loss in up to 68% of primary tumours (Yoshimoto et al. 2006; Yoshimoto et al. 2007) whereas following studies report *PTEN* deletion in about 15–20% of men that have undergone surgery (The Molecular Taxonomy of Primary Prostate Cancer 2015; Lotan et al. 2016). While *PTEN* loss

in primary prostate tumours is heterogeneous occurring only in some of the tumour cells, most or all cells in metastatic samples lack *PTEN* (Liu et al. 2009; Haffner et al. 2013) suggesting its role in invasiveness of the disease. Previous studies have shown that monoallelic *Pten* loss (*Pten+/–*) in mouse models induces PIN but does not lead to invasive prostate tumours while biallelic *Pten* loss (*Pten–/–*) in mice results in progression to invasive disease (Trotman et al. 2003).

Fig. 3 depicts the diverse roles of *PTEN* as a tumour suppressor. The lipid phosphatase activity of *PTEN* helps to convert phosphatidylinositol 3,4,5-trisphosphate (PIP3) into phosphatidylinositol 4,5-biphosphate (PIP2) (Maehama and Dixon 1998) and thus directly antagonise the function of class I phosphoinositide 3-kinase (PI3K), which converts PIP2 to PIP3. The negative regulation of PIP3 by *PTEN* results in tumour suppressive inhibition of serine/threonine-protein kinase AKT and mTOR signalling cascades. The AKT signalling pathway plays an important role in regulating cellular behaviors such as cell growth, proliferation, survival, and migration (Manning and Cantley 2007). *PTEN* also has a weak protein phosphatase activity inhibiting focal adhesion kinase 1 (FAK) and proto-oncogene tyrosine-protein kinase SRC (Zhang et al. 2011). Additionally, *PTEN* was shown to play a role in the nucleus localizing to centromeres and hence protecting their stability (Shen et al. 2007).

Loss/inactivation of *PTEN* causes accumulation of PIP3 on the cell membrane and this results in mobilization and activation of 3-phosphoinositide-dependent protein kinase 1 (PDK1) and AKT as its substrate. Phosphorylation of AKT activates the protein and thus its downstream signalling targets, such as mTOR. AKT/mTOR signalling regulates many cellular processes such as apoptosis, cell cycle progression, proliferation, metabolism, differentiation, and invasion (Song et al. 2012).

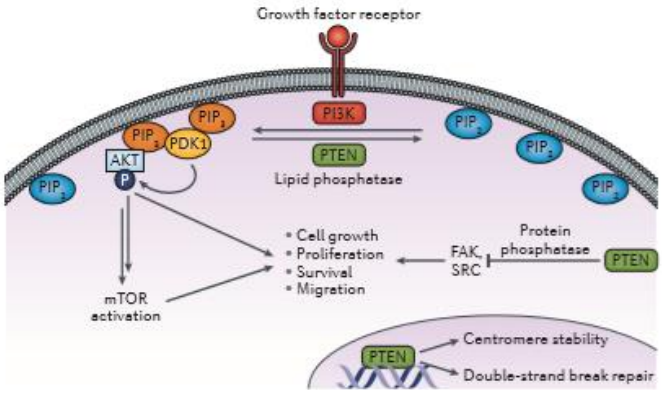

Figure 3
The various roles of *PTEN* (Jamaspishvili et al. 2018).

2.6.2 *P53*

P53 is classified as a tumour suppressor gene and is known by many as 'The Guardian of the Genome' for its role in cancer prevention. First strong evidence for the role of *P53* as a tumour suppressor was provided by studies in *Tp53*-knockout mice, which were shown to develop 100% penetrant, spontaneous tumours (Donehower et al. 1992; Jacks et al. 1994; Purdie et al. 1994). In humans, *P53* is located on the short arm of chromosome 17. It belongs to the genes that are mutated in over 50% of human cancers (Baker et al. 1989; Nigro et al. 1989; Takahashi et al. 1989; Vogan et al. 1993; Kelman et al. 1989). Mutation frequency of 25% of *P53* in PCa was reported (Schlechte et al. 1997). In patients after needle biopsy and those diagnosed with primary benign disease, these mutations were shown to shorten cancer free survival time (Ecke et al. 2007). *P53* loss is also generally associated with more aggressive tumours and progression of malignancy.

There are several mechanisms that underlie *P53*-mediated tumour suppression as shown in Fig. 4. For instance, *P53* gets activated upon acute DNA damage such as double strand breaks or instability of DNA replication forks by activation of the proteins ataxia-telangiectasia mutated (ATM) or ataxia telangiectasia and RAD3-related (ATR) (Kastan and Bartek 2004). Phosphorylation and thus stabilization of *P53* leads to interaction of *P53* with transcriptional regulators, which can further promote activation of target genes involved in different cellular processes such as cell cycle arrest, DNA repair, apoptosis and senescence (Jenkins et al. 2012).

In a similar manner, hyperproliferative signals stimulate transcriptional activation of the ARF tumour suppressor, which consequently inhibits MDM2. MDM2 as a negative regulator of *P53* enhances *P53* stability and activity and hence its downstream signalling as a tumour suppressor (Bates et al. 1998).

Recently, new evidence suggested various new players and processes in the tumour suppression pathway, for instance nutrient deprivation, hypoxia and oxidative stress as mean of triggers of activation of *P53* as well as regulation of cellular metabolism, stem cell function, invasion and communication between cells in the tumour micro environment as additional adverse tumour suppressive effects regulated by *P53* (Vousden and Prives 2009).

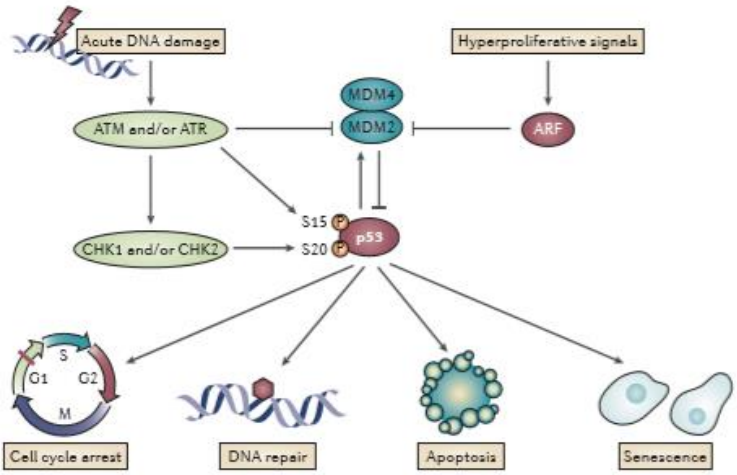

Figure 4
The signalling pathways of p53 activation and response (Bieging et al. 2014).

2.6.3 *STAT3*

STAT3 was identified to play a role in metastatic progression of different cancer entities such as lung, skin, liver, ovarian, kidney, and colon cancer (Li et al. 2006; Silver et al. 2004; Kusaba et al. 2005; Dauer et al. 2005) through different molecular mechanisms. Activation of *STAT3* was also shown to be associated with advanced PCa and it is believed to stimulate metastasis. It has been demonstrated that *STAT3* is active in 77% of lymph nodes and 67% of bone metastasis in patients suffering from PCa (Abdulghani et al. 2008). Although from the research that has been carried out, hyperactivity of *STAT3* in PCa was thought to be oncogenic (Mora et al. 2002; Horinaga et al. 2005), targeting it as a form of therapy did not provide expected outcome (Johnson et al. 2018). Recently, contradictory results were published where loss of *STAT3* or *IL-6* stimulates the progression to metastatic PCa in the *Pten* knockout mouse model. In this study, a novel direct *STAT3* target – ARF - was identified and the disruption of the ARF-MDM2-P53 tumour suppressor signalling pathway lead to bypassing senescence and thus cancer progression leading to metastasis (Pencik et al. 2015a).

Fig. 5 represents the signalling pathway of *STAT3.* Phosphorylation of a tyrosine residue in the carboxy-terminal domain of *STAT3* leads to *STAT3* activation and subsequently to its homodimerization and translocation to the nucleus. *STAT3* regulates transcription by binding to specific

STAT3 response elements of target gene promoters (Levy and Darnell 2002). *STAT3* is strongly associated with interleukin-6 (IL-6), which plays a role as a signal transducer and activator of *STAT3* signalling. IL-6 belongs to a family of cytokines and is involved in the

regulation of immune responses and inflammation (Schaper and Rose-John 2015) in various cancers, including PCa. Impaired signalling of IL-6/STAT3 in connection with loss of *P53* was shown to occur during PCa progression to metastatic disease (Pencik et al. 2015b).

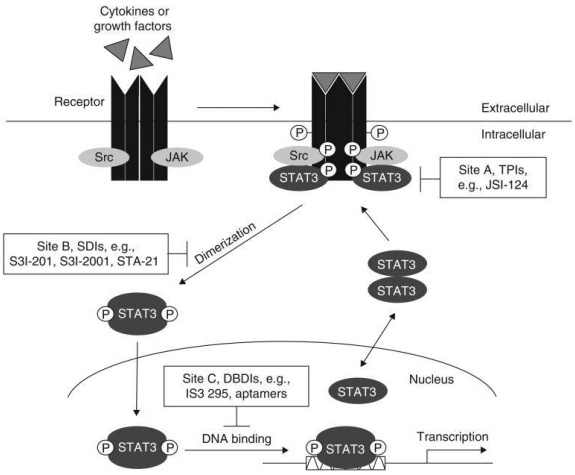

Figure 5
The upstream and downstream signalling pathways of *STAT3* (Yue and Turkson 2009).

3 Current model systems to study PCa

3.1 Cell lines

Most *in vitro* research on prostate biology and PCa is performed using cell lines. In spite of the high incidence of PCa, PCa cells have proven to be very difficult to isolate and successfully transfer to tissue culture. There are only a few cell lines in public repositories available for research. The most widely used cell lines are PC3 (Kaighn et al. 1978), LNCaP (Horoszewicz et al. 1983), and DU145 (Stone et al. 1978), each with a number of studies published. It remains unclear what factors influence the difficulty of culturing PCa cells *in vitro*.

3.2 Mouse models

The prostate is found only in mammals and its anatomy varies significantly between species (Marker et al. 2003). In spite of differences to human prostate, mouse model systems due to several advantageous assets such as small body size, uncomplicated breeding, resemblance between the human and mouse genome and easy genetic manipulation, have

been commonly used to study prostate biology (Cunha et al. 1987; Donjacour and Cunha 1988; Lamm et al. 2001) as well as PCa (Irshad and Abate-Shen 2013; Grabowska et al. 2014; Wu et al. 2013).

3.2.1 Mouse versus human prostate anatomy

Mouse prostate consists of four lobes – anterior, dorsal, ventral and lateral – surrounding the urethra as depicted in Fig. 6. Each lobe has specific characteristics such as the final shape of the lobe and histological features. The anterior prostate (AP) shows extensive epithelial-infolding, whereas the epithelial-infolding is significantly reduced in the dorso-lateral prostate (DLP) and near to invisible in the ventral prostate (VP) (Sugimura et al. 1986).

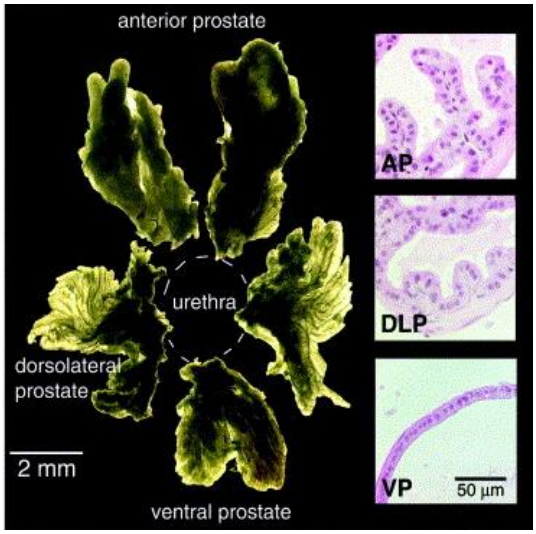

Figure 6
The lobes of the adult mouse prostate together with HE stained sections. (AP=anterior prostate; DLP=dorso-lateral prostate; VP=ventral prostate). Each lobe has a specific appearance (Marker et al. 2003).

In contrary to mice, the human prostate is a more compact organ and does not possess any exterior lobes as seen in Fig. 7. It consists of three regions so called peripheral zone (PZ), a central zone (CZ), and a transition zone (TZ). These individual regions reflect the three distinct prostatic ducts (J.E. McNeal 1983). The majority of prostate adenocarcinomas (75-85%) occur in PZ (McNeal et al. 1988; NOGUCHI et al. 2000) which is the homologous counterpart of the mouse DLP based on comparisons of mRNA expression

(Berquin et al. 2005). The CZ is hypothesized to be the human homologue of the mouse AP whereas the TZ is human-specific (Roy-Burman et al. 2004).

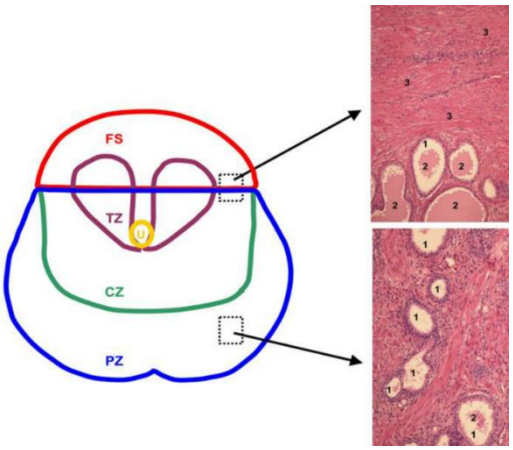

Figure 7
The regions of the adult human prostate and corresponding HE stained sections.
(PZ = peripheral zone; TZ = transition zone, CZ = central zone) (McNeal et al. 1988).

Even though the gland morphology varies between human and mice, the organization at the cellular level remains similar. The prostate epithelium consists of three primary cell types – luminal cells, basal cells and rare neuroendocrine cells as illustrated in Fig. 8. In both species, the secretory luminal cells form an epithelial layer surrounding the prostatic lumen into which they secrete prostatic proteins and fluids. Basal cells make a continuous surface layer in humans, while in mice, they are dispersed around the ducts mostly as single cells due to an overall fewer number of basal cells. Neuroendocrine cells are rare in both species and are present as single cells within the epithelial layer (Hudson 2004; Peehl 2005; Shappell et al. 2004; van Leenders and Schalken 2003). The different cell types can be distinguished by staining of various proteins. Cytokeratin (CK) 8, CK 18 as well as high levels of AR mark the secretory luminal cells, whereas the basal cells express CK 5, CK 14 and p63. Neuroendocrine cells express endocrine markers such as chromogranin A and synaptophysin.

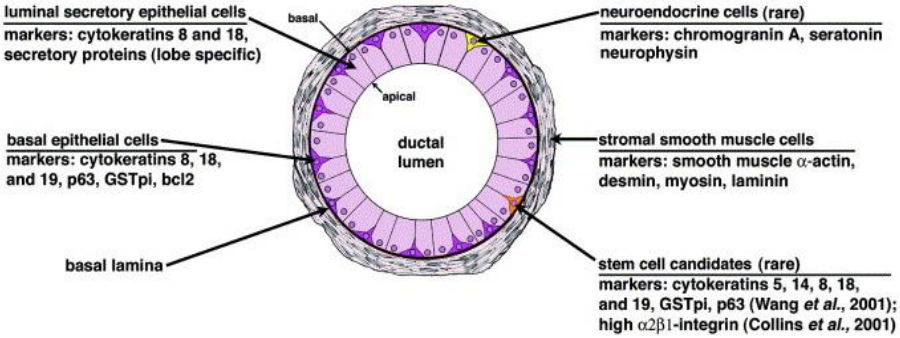

Figure 8
A diagram of a prostatic ductal cross-section with labelled cell types and their differentiation markers (Marker et al. 2003).

3.2.2 Characterization of mouse models used in this study

3.2.2.1 Pten$^{fl/fl}$;PB-Cre4 (Pten$^{pc-/-}$)

Pten$^{loxp/loxp}$ (Lesche et al. 2002) mice were crossed with *ARR2Probasin-Cre* transgenic line - PB-Cre4 (Wu et al. 2001) – to obtain deletion of *Pten* in the prostate tissue. The deletion was shown to vary between prostate lobes but was near to 100% completed at the age of 8 months. Homozygous *Pten* deletion led to enlarged prostate glands, from 4 weeks on to hyperplasia, from 6 weeks on to murine PIN (mPIN) and to invasive prostate adenocarcinoma by 9 weeks of age (Wang et al. 2003). In contrast, mPIN formation in heterozygous mice began earliest from 8 months of age. Additionally, 5 out of 11 *Pten* homozygous knockout mice displayed lymphovascular invasion from 12 weeks of age, which further progressed over time into distance metastasis found in the lymph nodes and lung. Hence, this study indicates that *Pten* loss is sufficient to initiate development of PCa and also metastasis.

3.2.2.2 *Pten$^{fl/fl}$Tp53$^{fl/fl}$*;PB-Cre4 (*Pten$^{pc-/-}$;Tp53$^{pc-/-}$*)

Pten and *Tp53* prostate-specific deletion was achieved by crossing female *Pten$^{loxP/loxP}$*; *Tp53$^{loxP/loxP}$* with male PB-Cre4 mice as described previously (Wu et al. 2001).

As mentioned above, *Pten* deletion alone drives early onset tumorigenesis. Another study demonstrated that all three prostate lobes possess high-grade PIN (HG-PIN) upon *Pten* loss at 9 weeks of age. In contrast, authors emphasize that whereas *Tp53* deletion did not lead

to any pathological changes at the same age, combination of *Pten* and *Tp53* inactivation in the prostate did cause HG-PIN in all *Pten* and *Tp53* deficient mice. In 50% of those, HG-PIN progressed to invasive cancer and metastasis by 10 weeks of age. Besides, tumour weight in double knockout mice increases 32-fold compared to tumours in *Pten* single knockout mice causing them to invade the whole genitourinary tract and pelvis. Hence, on the contrary to loss of *Pten* alone, evidence suggests that *Tp53* deletion does not cause the onset of malignancy but speeds up tumorigenesis that was initiated by loss of *Pten* (Chen et al. 2005).

3.2.2.3 *Pten*$^{fl/fl}$*Stat3*$^{fl/fl}$;PB-Cre4 (*Pten*$^{pc-/-}$;*Stat3*$^{pc\ -/-}$)

Pten and *Stat3* prostate-specific deletion was achieved in similar manner as previously described (Wu et al. 2001).

The literature investigating effects upon *Pten* and *Stat3* loss in a prostate mouse model are controversial and inconsistent. One study demonstrated reduced tumour size by about 70% in *Pten*$^{pc-/-}$*Stat3*$^{pc-/-}$ mice at late stages of tumorigenesis compared to *Pten*$^{pc-/-}$ mice as well as reduced rate to only 25% of tumours progressing into invasive cancer upon *Pten*$^{pc-/-}$*Stat3*$^{pc-/-}$ loss compared to 100% of *Pten*$^{pc-/-}$ mice developing invasive PCa at the later stages of the disease (Toso et al. 2014).

However, Pencik *et. al* surprisingly presented contradictory results. Their data displayed enhanced PCa development that led to tumours up to six-fold larger in size in *Pten*$^{pc-/-}$*Stat3*$^{pc-/-}$ mice in comparison to *Pten*$^{pc-/-}$ mice at 52 weeks of age. Also, according to their results, 75% of *Pten*$^{pc-/-}$*Stat3*$^{pc-/-}$ mice developed metastasis that spread to liver and lungs whereas in *Pten*$^{pc-/-}$ mice, the tumour cells invaded only the surrounding tissue - the seminal vesicles. Additionally, the lifespan of *Pten*$^{pc-/-}$*Stat3*$^{pc-/-}$ mice was significantly reduced when compared to wildtype mice (Pencik et al. 2015a).

The role of *Stat3* in *Pten*-deficient mice remains controversial and further research is needed to clarify the role of *Stat3* in this mouse model.

3.3 Organoid technology

Organoids are by definition a 3D model of an organ that was derived from pluripotent, neonatal or adult stem cells, in which these cells self-organize and differentiate in a manner

comparable to *in vivo* and which recapitulates at least some organ-specific functions (Fig. 9) (Lancaster and Knoblich 2014; Huch and Koo 2015).

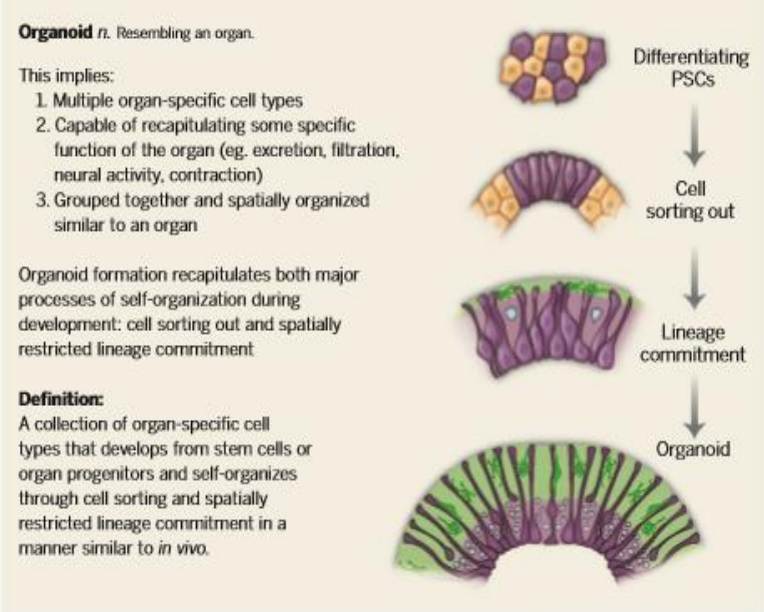

Figure 9
Definition of organoids (Lancaster and Knoblich 2014).

This novel emerging *in vitro* system has been one of the biggest scientific breakthroughs of the last decade. Even though the first glimpse of this scientific achievement dates back to 1907 already, when the first dissociation-reaggregation experiments started and the potential to self-organize after dissociation of sponge cells was discovered (Wilson 1907). These experiments were followed further by experiments in chick embryos and other model organisms. In the 1960s studies have shown the potential to recapitulate complete renal development in disassociated cells from the developing chick kidney (Weiss and Taylor 1960).

It is indeed the ability to self-organise that is the foundation of organoid formation. Self-organisation in organoids was made possible by embedding the cells into an extracellular matrix, for instance the laminin-rich Matrigel secreted by the Engelbreth-Holm-Swarm tumour line (Li et al. 1987). Especially primary cells and stem cells need the support of the extracellular matrix in combination with a defined culture medium to remain in an undifferentiated state. Matrigel is a gelatinous protein mixture that solidifies at 37°C

creating a 3D structure that supports the growth, maintenance and differentiation of a variety of cells (Kleinman and Martin 2005) .

There are several organoid lines successfully established from human pluripotent stem cells from kidney, colon, brain, retina and many more. Several publications have appeared in recent years documenting the progress of developing prostate organoid cultures. The culture conditions previously used to establish other organoid systems such as colon organoids (Sato et al. 2011) were optimized to allow the growth of prostate cells in a 3D culture. Gao et al. and Chua et al. presented prostate organoids derived from prostate metastasis biopsies, circulating tumour cells and primary prostate. Nevertheless, the efficiency of establishing those lines was rather low and they were only successfully maintained in culture for up to maximum 2 months (Gao et al. 2014; Chua et al. 2014). In 2016, a protocol describing a step by step set up of 3D prostate organoid cultures from a healthy mouse and a human prostate, metastatic prostate cancer lesions and circulating tumour cells was published. These cultures harbor both luminal and basal cell lineages, have functional AR signalling, can be propagated as long term cultures and resemble genetically and phenotypically the tissue they were obtained from (Drost et al. 2016). Human primary PCa organoids have not been successfully established as long term cultures so far.

4 Materials and Methods

4.1 Cell culture methods

4.1.1 Murine prostate culture medium (PCa medium)

The murine prostate organoids were cultured in PCa medium. Hepes, penicillin/streptomycin (PenStrep) and GlutaMAX were added into basal adMEM medium and stored at 4°C. PCa medium was prepared fresh approximately every 2 weeks (or depending on necessity) by adding several factors listed in the table below together with their respective concentrations into basal adMEM medium (containing Hepes, PenStrep and GlutaMAX).

Table 1: Composition of PCa medium

	Amount	Final concentration
adMEM (Life Technologies, 12634-010) + 10 mM Hepes (Life Technologies, 15630056), 1% PenStrep (Life Technologies, 15140122), 100x diluted GlutaMAX (Life Technologies, 35050061)	48.2 ml	
50x B27 (Life Technologies, 17504-001)	1000 µl	1 x
1 M Nicotinamide (in PBS) (Sigma-Aldrich, N0636)	500 µl	10 mM
500 mM N-Acetylcystein (in PBS) (Sigma-Aldrich, A9165-5G)	125 µl	1.25 mM
1 µM DHT (in ethanol) (Sigma-Aldrich, A8380-1G)	50 µl	1 nM
10 mM y27632 (Selleck Chemicals, HY-10583)	50 µl	10 µM
0.5 mg/ml EGF (in PBS + 0.1% BSA) (PeproTech Austria, AF-100-15)	5 µl	0.05 µg/µl
500 µM A83-01 (in DMSO) (Sigma-Aldrich, SML0788-5MG)	20 µl	200 nM

4.1.2 Generation of mouse organoid cultures from healthy/tumour prostate tissue

Isolated murine prostate healthy/tumour tissue containing anterior and dorsal lobes was cut into about 1 mm^3 pieces in a 10 cm culture dish. The cut prostate pieces were resuspended in 500 µl of PCa medium additionally containing 5 mg/ml Collagenase 2 and 10 µM Y-2763 and transferred into a 1,5 ml Eppendorf tube. The sample was left to digest for 2 h at 37°C on a shaking platform. Afterwards, the sample was centrifuged at 300 x g

for 5 min at 4°C. Supernatant was carefully removed and the pellet was resuspended in 500 µl TrypLE with 10 µM Y-27632 and left to digest again for 15 min at 37°C on a shaking platform. The solution was put through a 40 µm cell strainer into a 50 ml falcon tube. The cell strainer was washed twice with 2 ml 1xPBS in order to collect all remaining material. The solution was centrifuged at 150 x g for 5 min at 4°C. The supernatant was discarded, and the pellet was dissolved in an appropriate amount of Matrigel depending on the pellet size and plated in a pre-warmed 24 well plate. The plate was inverted to prevent adherence of cells to the plate bottom and placed into the 37°C incubator for 15 min to allow Matrigel to solidify. 500 µl of pre-warmed PCa medium was added and refreshed every 2 days.

4.1.3 Passaging of murine prostate organoid cultures

PCa medium was removed from the wells and samples were washed with 500 µl PBS. 250 µl Trypsin were added, samples were pipetted up and down several times and put into a 37°C incubator for 5 min. The cells were checked under the microscope and trypsinized for additional several minutes if needed to achieve single cell suspension. Additionally, cell suspension was passed through a 27G needle if needed. Single cell suspension was added into a 15 ml falcon tube containing 5 ml PBS and 5 µl Y-27632 (10 µM) and centrifuged for 5 min at 250 x g. Supernatant was removed and cells were plated as described.

4.1.4 Cryopreservation of murine prostate organoid cultures

PCa medium was removed from the samples. Each Matrigel drop was dissolved in 1 ml basal adMEM medium (Hepes, PenStrep and GlutaMAX added) additionally containing 10% DMSO and transferred into a labelled cryo tube. The cryo tubes were placed into a cool cell and put into a -80°C freezer. Samples were transferred into a liquid nitrogen tank for long term storage.

4.1.5 Thawing of murine prostate organoid cultures

Samples frozen in liquid nitrogen were placed into a water bath for approximately 5 min. When thawed fully, samples were transferred into a 15 ml falcon tube containing 5 ml pre-warmed basal adMEM medium (Hepes, PenStrep and GlutaMAX added) and 5 µl Y-27632 (10µM). Samples were centrifuged for 5 min at 250 x g. Supernatant was removed and cells were plated as described.

4.1.6 Embedding of murine prostate organoid cultures

The PCa medium was removed from the wells and Cell recovery solution was added. The Matrigel drops were gently resuspended in the Cell recovery solution, transferred into BSA coated Falcon tubes and rotated on a platform for 40 min at 4°C in order to dissolve remaining Matrigel. 7 ml of PBS were added into the Falcon tubes and the samples were centrifuged for 5 min at 250 x g. The supernatant was removed, the samples were resuspended in 8 µl of Matrigel and plated in a 6-well plate. The plate was placed into the 37°C incubator for 15 min to allow Matrigel to solidify and then incubated for 5 min at room temperature to cool down. The drops were covered with room temperature 4% PFA (in PBS) for 10 min. The PFA solution was removed and the samples were washed in 3 washes of PBS for 5 min each. The samples were further dehydrated by incubation in different solutions as follows: 2 washes of 70% ethanol for 1 h each, 2 washes of 80% ethanol for 1 h each, in 2 washes of 95% ethanol for 1 h each, in 3 washes of 100% ethanol, for 1h each, in 3 washes of xylene for 1h each and 2 washes of paraffin wax (56-58ºC) for 1,5 h each. Samples were cut, mounted and stored in a plastic chamber for further use.

4.2 Genetic engineering methods

4.2.1 Plasmid amplification and preparation

4.2.1.1 Characterization of plasmids

The MSCV CreERT2 puro plasmid was used to generate tamoxifen inducible *in vitro* knockout of *Pten* and a double knockout of *Pten* and *Stat3*. The plasmid contains a fusion between the Cre-recombinase and the estrogen receptor, making it inducible upon tamoxifen or its derivate 4-hydroxytamoxifen (4-OHT) treatment. Puromycin resistance is used for selection. A control version of this plasmid (CreCut) was created in which the Cre-recombinase gene is shortened and thus not functional. The plasmid maps of both plasmids are shown in Figs. 10 and 11 and additional information about the plasmids is summarized in Table 2.

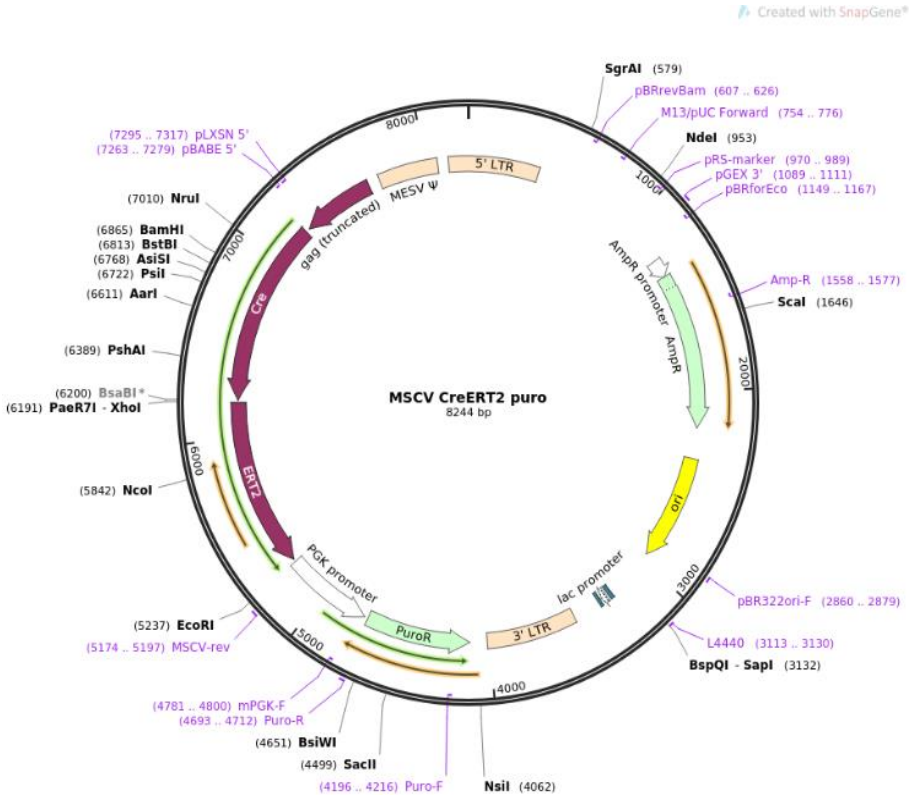

Figure 10
Plasmid map of MSCV CreERT2 puro

Figure 11
Plasmid map of MSCV CreCut puro

Table 2: Characteristics of CreERT2 and CreCut puro plasmids

Plasmid	Backbone	Backbone size with insert (bp)	Type	Copy number	Bacterial strain	Selectable marker for E. coli	Selectable marker for mammalian cells
CreERT2	pMSCV puro	8244	Mammalian expression, Retroviral	Low copy	DH5-α competent E. coli	Ampicillin	Puromycin
CreCut	pMSCV puro	7574	Mammalian expression, Retroviral	Low copy	DH5-α competent E. coli	Ampicillin	Puromycin

4.2.1.2 Transformation of E.coli with MSCV CreERT2/CreCut puro plasmids

A tube of NEB DH5-α competent E.coli cells was thawed on ice for 10 min. 50 µl of E.coli cells were transferred into an Eppendorf tube and 1 µl of plasmid DNA was added to the cell mixture. The tube was gently flicked to mix cells and DNA and incubated on ice for 15 min. Cells were heat shocked for 30 s in a 42°C water bath and afterwards placed on ice for 5 min. 950 µl of room temperature S.O.C. medium (Invitrogen™) was added and samples were left to shake at 250 rpm at 37°C for 1 h. 100 µl of the transfected cells was spread on Agar plates containing Ampicillin. Agar plates were incubated overnight at 37°C. For further amplification and isolation of the plasmid, Maxi Kit from QUIAGEN was used following manufacturer's instructions.

The microbial cultures were grown in Luria-Bertani (LB) medium. The LB medium was autoclaved at 121 °C for 20 min after preparation and stored at 4°C for later use.

Table 3: Composition of Luria-Bertani medium

Luria-Bertani (LB) medium
1% w/v tryptone (Beckton Dickinson)
0.5% w/v yeast extract (Beckton Dickinson)
0.5% NaCl in ddH2O

4.2.2 Lentiviral transduction of murine organoid cultures

4.2.2.1 Transformation of PHOENIX-Eco with MSCV CreERT2/CreCut puro plasmids

In order to be able to perform the transduction, the MSCV CreERT2/CreCut puro vector needs to be packaged by the helper cell line PHOENIX-Eco. For the transfection of the vector into these cells, Lipofectamine 2000 (Invitrogen) was used. The cells were cultivated

in a 10 cm petri dish in DMEM medium (Gibco) to about 70% confluency. The medium was carefully changed for Opti-MEM medium (Gibco) prior the transfection. 60 µl of Lipofectamine were mixed with 500 µl of Opti-MEM in an Eppendorf tube. In parallel, 7 µg of the MSCV CreERT2 puro vector were mixed with 500 µl Opti-MEM. Both individual reaction solutions were incubated for 5 min at room temperature, then mixed and incubated further for 20 min at room temperature. After the incubation the reaction mix was added dropwise onto PHOENIX-ECO cells and the cells were incubated at 37°C for 24 h. Afterwards, the medium was changed for DMEM and the cells were incubated for another 24 h. Finally, the cells were centrifuged and the supernatant containing the viral particles was harvested.

4.2.2.2 Lentiviral transduction of murine organoid cultures with MSCV CreERT2/CreCut puro plasmid

A day prior to the transduction, organoids were passaged as single cell suspension as already described and plated in a 24-well plate as a 2D culture in 500 µl of PCa medium. The cells were incubated at 37°C for 24 h to attach to the bottom of the plate. The medium was exchanged for PCa medium without antibiotics, 4µg/ml Polybrene (Sigma) and 7 µl of viral supernatant was added. The solution was gently mixed by swirling the plate. The cells were incubated at 37°C for 24-48 h before plating them in Matrigel and adding the selection medium.

4.2.3 Electroporation of murine prostate organoid cultures

Approximately 6 dense drops of at least 200 µm large organoids were used per 1 electroporation.

PCa medium was changed a day prior to electroporation to PCa medium without antibiotics containing 1.25% DMSO. Organoids were trypsinized to small clusters of approximately 4 - 5 cells and transferred into a 15 ml falcon tube containing 5 ml PCa medium and 5 µl Y-27632 (10µM). Samples were centrifuged for 5 mins at 250 x g. Supernatant was removed and the cells were resuspended in 90 µl BTXpress buffer and 10 µl of 10 - 20 µg DNA. The cell - DNA mixture was added into a cuvette and placed into a cuvette holder of the NEPA21 electroporator. Impedance was measured and if between 30 – 55 mA, electroporation was performed according to conditions summarised in Table 4. After the electroporation, 400

µl Optimem medium was added to the cuvette and the whole volume was transferred to an 1,5ml Eppendorf tube. After incubation at room temperature for 30 min, samples were centrifuged at 250 x g for 5 min. Supernatant was removed and cells were plated as described. 500 µl of PCa medium without antibiotics and containing 1.25% DMSO was added. This medium was changed for a medium without DMSO a day after electroporation. 3 - 4 days after electroporation this medium was changed to usual PCa medium and the drug selection was started.

Table 4: NEPA21 electroporation conditions

	Poring pulse	Transfer pulse
Voltage	200V	20V
Pulse length	5 sec	50msec
Pulse interval	50msec	50msec
Number of pulses	2	5
Decay rate	10%	40%
Polarity	+	+/-

4.3 Molecular biology methods

4.3.1 DNA isolation

Cell pellets were resuspended in 500 µl of genomic DNA lysis buffer. 20 µg/ml of RNaseA were added and the samples were incubated for 1 h at 37°C. Afterwards 500 µg/ml of Proteinase K were added, and samples were incubated overnight at 55°C in a thermal shaker. Next day, the DNA isolation continued using phenol/chloroform extraction method. The samples were transferred to phase lock gel tubes (5 prime) and 500 µl of buffered phenol/chloroform was added. The solutions were mixed by inverting the tubes and centrifuged at 13 000 rpm for 10 min. The upper phase was transferred into a new Eppendorf tube and 1 volume of isopropanol was added. The solutions were shaken vigorously for 15 sec. Samples were centrifuged for at 13 000 rpm for 5 min. The supernatant was discarded, and the pellets were washed with 750 µl of 75% EtOH by pipetting up and down. Samples were centrifuged one more time at maximum speed for 3

min. The supernatant was removed, the pellets were air dried for 5 min and dissolved in 20 - 50 µl (depending on the pellet size) of ddH20. Lastly, samples were incubated for 1 h at 37°C. DNA concentrations were measured with Nanodrop 2000 spectrophotometer (Thermo Scientific).

Table 5: Composition of DNA lysis buffer

Genomic DNA lysis buffer
0,4 M NaCl
0,2% SDS
1M Tris
5 mM EDTA

4.3.2 RNA isolation

RNA was isolated using the RNeasy Mini Kit (QIAgen) according to the manufacturer's instructions. Prior to the isolation, the working area was cleaned with RNase AWAY Surface Decontaminant (Thermo Scientific). RNA concentrations were measured with Nanodrop 2000 spectrophotometer (Thermo Scientific).

4.3.3 PCR

DNA of transduced/transfected samples with Cre and CreCut vectors was isolated and amplified with PCR according to PCR conditions summarized in Table 6 and 7. PCR reaction (step 2 – 4) ran in 34 x cycles. The PCR products were run on a 1% agarose gel containing 1% midori green at 120V for 20 - 30 min. The bands of the PCR products were visualized with UV light.

Table 6: Composition of PCR reaction for 1 sample

General PCR set-up (15 µl reaction)	
GoTaq	7,5 µl
ddH20	5 µl
10 µM primer mix	1,5 µl
DNA template	1 µl

Table 7: PCR conditions for genotyping with Cre and CreCut plasmids

PCR conditions	
Cre	
94 °C	5 min
94°C	0,5 min
55°C	0,5 min
72°C	1 min
72°C	10 min
CreCut	
95°C	5 min
95°C	0,5 min
57°C	1 min
72°C	2 min
72°C	10 min

Table 8: Primer sequences

Primer sequences	
Cre_forward	5'-ATG CTT CTG TCC GTT TGC CG-3'
Cre_reverse	5'-TGA GTG AAC GAA CCT GGT CG-3'
CreCut_forward	5'-CGA CCA GGT TCG TTC ACT CA-3'
CreCut_reverse	5'-GGT TGG CAG CTC TCA TGT CT-3'

4.3.4 Protein isolation

Cells were centrifuged and resuspended in an appropriate amount (twice the size of the pellet) of HUNT lysis buffer. Samples were frozen in liquid nitrogen and thawed at 37°C for 30 sec. Then frozen again in liquid nitrogen and thawed on ice for 10 minutes. Samples were centrifuged at 16 800 rcf for 15 min at 4°C. The supernatant containing proteins was transferred into a new Eppendorf tube and the protein concentration was measured using a Bradford assay. Aliquots of the samples were stored at -80°C.

Table 9: Composition of HUNT buffer

HUNT buffer	
20 mM Tris (pH = 8,0)	800 µl
100 mM NaCl	660 µl
1 mM EDTA	80 µl
0,5 % NP-40	2 ml
ddH2O	fill up to 40 ml

4.3.5 Western blot analysis

7 µg of isolated protein were diluted in HUNT buffer and filled up to a final volume of 15µl with Laemmli buffer. The samples were incubated at 95°C for up to 10 min and then loaded onto a 10% polyacrylamide-gel. The proteins were separated by gel-electrophoresis using 0.02 mA as a constant. The separated proteins were blotted onto a nitrocellulose membrane from the gel during wet transfer. The transfer ran at 120V for 2 h at 4°C. The membrane was stained with Ponceau-red to visualize the proteins and then washed with 1x TBS-T for 5 min on a rocking platform. The membrane was blocked with a blocking solution for 1 h. Afterwards the primary antibody diluted in blocking solution was applied onto the membrane for an incubation over night at 4°C. Next day the membrane was washed 4 x for 5 min with 1xTBS-T on a rocking platform and secondary antibody diluted 1:10 000 in 1 x TBS-T was applied for 1 h at room temperature. Membrane was washed again 4 x for 5 min with 1x TBS-T. Protein signal was measured with LumiAnalyst imager (Roche) using ECL plus Western blotting reagent (Thermofisher).

Table 10: Composition of solutions used for Western blot

10 x TBST-T buffer	
Tris	60,5 g
NaCl	90 g
Tween-20	0,10%
H2O	fill up to 1 l
4x Laemmli buffer	
Tris (1.0 m, pH 6.8	1 ml
SDS	4 mg
Glycerol	2 ml
β-Mercaptoethanol	1 ml
Bromophenol blue	0.1 mg
ddH2O	fill up to 5 ml
Electrophoresis buffer	
Glycine	14,4 g
Tris	3 g
SDS	1 g
H20	Fill up to 1 l
Transfer buffer	
Glycine	2,46 g
Tris	200 ml
Methanol	Fill up to 1 l
Blocking solution	
Instant milk powder	25 g
NaN3	0,01%
1xTBS-T	fill up to 500 ml

Table 11: Composition of SDS-polyacrylamide gels

Gels for SDS-polyacrylamide electrophoresis		
	10% separating gel (15 ml)	5% stacking gel (5 ml)
H2O	5,9 ml	3,4 ml
30% acrylamide mix	5 ml	830 µl
1,5 M Tris pH = 8.8	3,8 ml	/
1 M Tris pH=6,8)	/	630 µl
10% SDS	150 µl	50 µl
10% APS	150 µl	50 µl
TEMED	6 µl	5 µl

Table 12: List of antibodies used for Western blot

Primary antibodies	Provider	Dilution
PTEN	Abcam (ab31392), rabbit mAb	1:1000
STAT3	Cell signaling (12640), rabbit mAb	1:1000
pSTAT3	Cell signaling (9131), rabbit mAb	1:1000
AKT	Cell signaling (4691) rabbit mAb	1:1000
pAKT	Cell signaling (9271) rabbit mAb	1:1000
β-ACTIN	Abcam (ab8227), rabbit mAb	1:5000
Secondary antibodies		
Goat Anti-Rabbit IgG	Abcam (ab205718)	1:10000

4.4 Immunohistochemistry (IHC)

Firstly, the embedded tissue requires to be deparaffinized and rehydrated. The slides with paraffin embedded organoids were placed in a rack and put into a 56°C incubator for 2 h. Afterwards the sections were incubated in 2 washes of xylene for 10 min each, in 2 washes of 100% ethanol for 3 min each, in 1 wash of 96% ethanol for 3 min, in 1 wash of 70% ethanol for 3, in 1 wash of 50% ethanol for 3 min and lastly, in 2 washes of dH20 for 5 min each. The citrate buffer was used for antigen retrieval. The slides were put into a plastic chamber filled with the citrate buffer and autoclaved. To cool off the slides, they were incubated for 20 min at room temperature. Afterwards they were rinsed in PBS several times, blocked in 3% hydrogen peroxide for 10 min to reduce nonspecific background staining and washed in PBS again. The slides were put into a humid chamber to prevent drying of the slides. Mouse blocking reagent was applied, and the slides were incubated for 1 h at room temperature. The slides were rinsed in PBS to remove the blocking solution, primary antibody diluted in 1% BSA were applied and the samples were incubated overnight at 4°C. Next day, the slides were washed 4 times in PBS for 3 min each. For the detection, UltraVision LP Large Volume Detection System from Thermo Scientific was used. Primary Antibody Enhancer was applied, and samples were incubated for 10 min at room temperature. Next, HRP Polymer was applied and the samples were incubated in the dark for 15 min at room temperature. Slides were washed 4 times in PBS for 3 min each. AEC

chromogen was applied, and the developing staining was closely monitored. As soon as the staining developed, the reaction was stopped by putting the slides into dH20. Finally, the slides were counterstained in hematoxylin for 30 sec, washed in dH20 and the coverslips were mounted with Aquatex (Sigma-Aldrich).

Table 13: List of antibodies used for IHC

Primary antibodies	Provider	Dilution
Ki67	Abcam (ab16667) rabbit mAb	1:500
STAT3	Cell signaling (9139), mouse mAb	1:300
CK8	Abcam (ab137855), rabbit mAb	1:200
pAKT	Cell signaling (3787) rabbit mAb	1:50

4.5 Immunofluorescence (IF)

The PCa medium was removed from the wells and the organoids were resuspended in cell recovery solution to dissolve remaining Matrigel as previously described. Samples were centrifuged for 5 min at 250 x g. The pellet was resuspended on ice in a suitable amount of Matrigel and diluted with cold 1x PBS in various ratios (dilution 1:3: 45 µl Matrigel were added to the pellet, mixed by pipetting and diluted with 130 µl PBS). 25 µl of the dilution mix were evenly distributed at the bottom of each well of a chamber slide without touching the chamber walls. The solution was dried at 37 °C for 5 min. From this step onwards, all solutions were pipetted along the chamber walls carefully to not disturb the embedded organoids and the slide was kept at room temperature gentle shaking (54 rpm) unless otherwise stated. Organoids were overlaid with fixation solution 1 for 20 min (no shaking), followed by incubation in fixation solution 2 for 30 min. The wells were washed in 3 washes of washing buffer (400 µl/well) for 10 min each and permeabilized with permeabilization buffer for 30 min. The washing steps were repeated. Samples were overlaid with 300 µl blocking buffer for 30 min. Samples were incubated with 150 µl primary antibody solution diluted in blocking buffer over night at 4 °C under gentle shaking. (The chamber slide was carefully sealed with parafilm and the incubation took place in a humid chamber). Next day, wells were washed in 3 washes with 400 µl washing buffer for 15 min each and incubated with 150 µl secondary antibody diluted in blocking solution in the dark for 2 h. The washing steps were repeated while keeping the samples in the dark and finally, the

organoids were incubated with DAPI for 20 min. Samples were shortly rinsed with washing buffer and the chamber was removed. The slide was dried by carefully soaking up remaining liquid with a tissue. The samples were mounted with Fluoprep Mounting medium and covered with a cover glass. The slide was dried at room temperature for 15 min and stored at 4 °C. Prior to imaging, the slide was warmed to room temperature. The samples were imaged with a LSM5 Exciter (Zeiss) following these settings: excitation at 405 nm (DAPI), 488 nm (Alexa Fluor 488) and 543 nm (Alexa Fluor 594) with laser intensities <30 % and a pinhole <50 µm.

Table 14: List of antibodies used for IF

	Provider	Dilution
Primary antibodies		
Ki67	Abcam (ab16667), rabbit mAb	1:200
CK14	Abcam (ab51054), rabbit mAb	1:300
Secondary antibodies		
Goat Anti-Rabbit IgG	Abcam (ab205718)	1:4000

Table 15: Composition of solutions used for IF

Fixation solution 1	
PFA	4%
PBS	1x
Fixation solution 2	
PFA	4%
PBS	1x
Triton-X 100	0,10%
Washing buffer	
PBS	1x
Triton-X 100	0,10%
Tween	0,05%
Permeabilization buffer	
PBS	1x
Triton-X 100	0,50%
Blocking buffer	
PBS	1x
Triton-X 100	0,10%
Goat serum	10%

5 Results

5.1 Generation of murine prostate organoid cultures

Murine prostate organoids of benign and malignant origin were derived from healthy prostate tissue of wildtype Cre-negative mice with floxed alleles and tumour tissue of transgenic mice harbouring different genetic knockouts of PCa relevant genes such as *Pten* and combination of *Pten/Stat3* and *Pten/Tp53* genes. The tissue of origin was digested, and the cells were brought into 3D culture as described in the previous chapter (4.1.2). The organoids were split every week depending on the density and cultured for several passages in PCa medium. The culture conditions eliminated contamination with other type of cells such as immune cells and led to pure prostate organoid cultures. A panel of biological triplicates of each genotype was established. Fig. 12 shows representative brightfield images of each genotype. Generally, the morphology of the organoids within each organoid line can vary depending on the seeding density, proliferation rate of each cell type, availability of different factors in the culture medium and others.

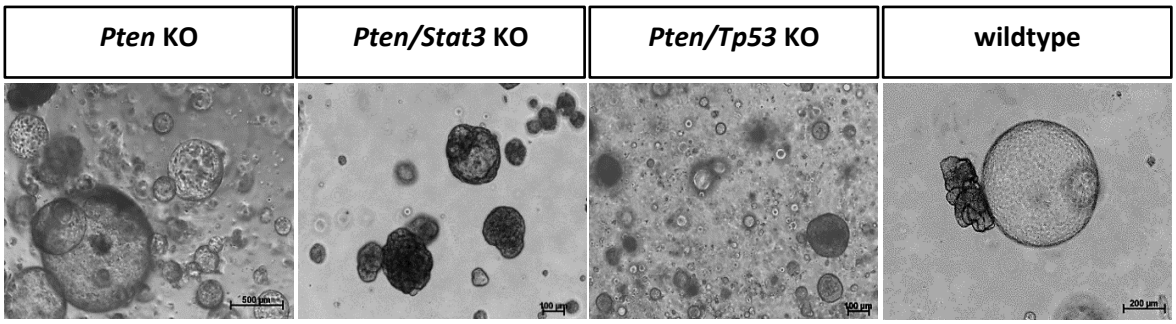

Figure 12
Brightfield images of *Pten*, *Pten/Stat3*, *Pten/Tp53* knockout organoids and the wildtype control. (Scale bars/Magnification: *Pten* KO ▬ 500 µm/4X; *Pten/Stat3* KO, *Pten/Tp53* KO and wildtype ▬ 200 µm/10X.)

5.2 Characterization of murine prostate organoids of different genetic background

5.2.1 Histo-morphological characterization

The organoids and the tissue of origin were further embedded and stained with Hematoxylin and Eosin (HE). HE staining is the gold standard of the principal tissue stains

that are used for medical diagnosis in histology (Titford 2005). Figure 13 portrays the HE stained tumour tissue for each genotype, healthy prostate tissue of wildtype mice and organoids derived from the corresponding tissue. While the healthy prostate tissue represented classical epithelial lined prostate glands, the structure of these glands was deeply impaired in the tumours. The organoids derived from the corresponding tissue highly retained the microscopic features seen in the original tissue. While the majority of wildtype organoids possessed an outer epithelial layer and an inner lumen resembling healthy prostate glands, most of PCa organoids showed tightly packed inner layers with a small or no lumen. The outer layer of the tumour organoids also often had multi-lobulated structures. The morphological differences in the original tumour tissue between the knockouts was also mirrored in the corresponding organoid lines.

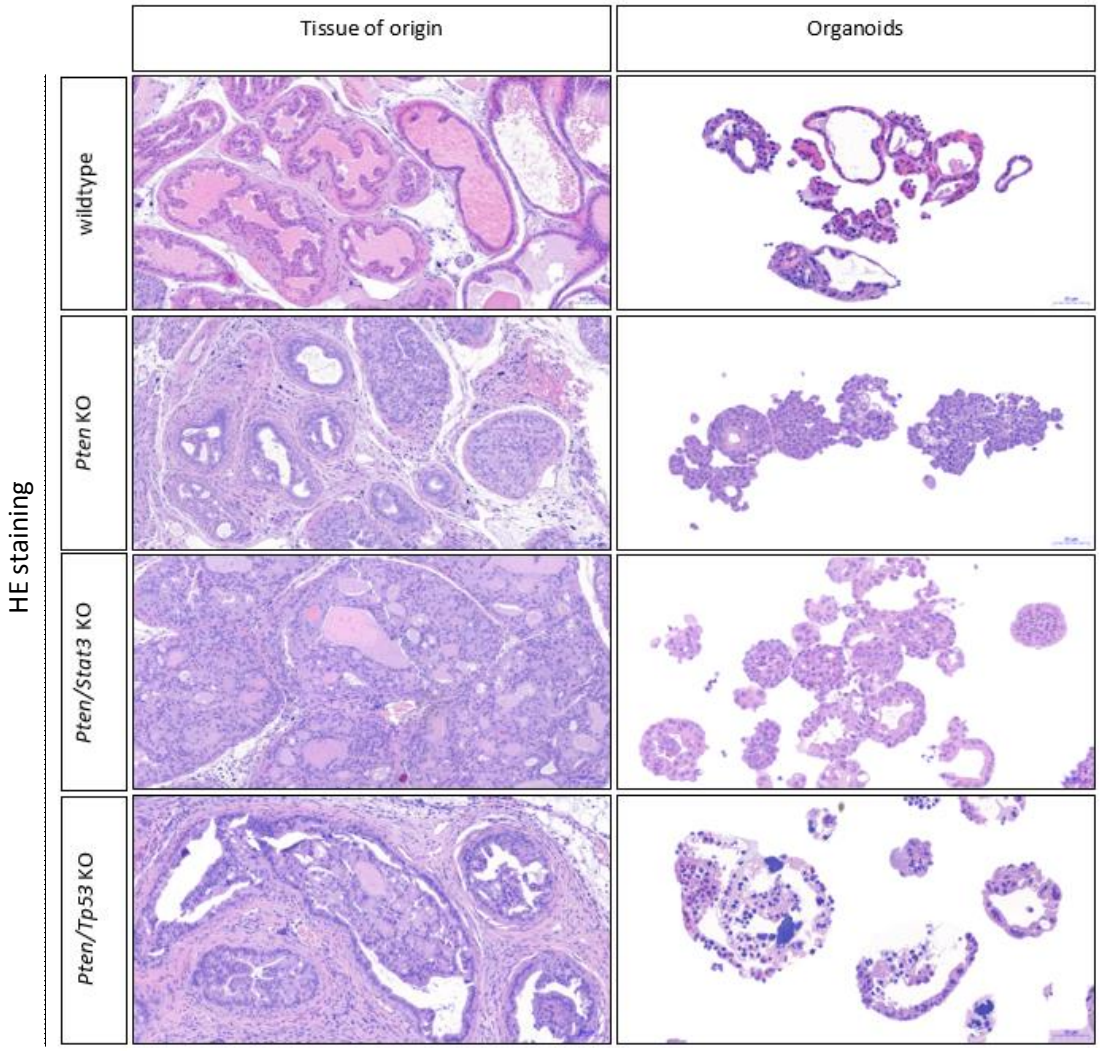

Figure 13
Comparison of murine HE stained tissue of origin of *Pten, Pten/Stat3, Pten/Tp53* and wildtype tissue and organoids derived from the corresponding tissue. (Scale bars/Magnification: Tissue of origin ▬ 100 µm/10X; Organoids ▬ 50 µm/20X.)

5.2.2 Characterization of proliferation

Ki67 is a protein that is present during active phases of the cell cycle (G_1, S, G_2, and mitosis), but is not detectable in resting cells (G_0). It is therefore used as a cellular marker for proliferation (Scholzen and Gerdes 2000). Ki67 was previously shown to be significantly upregulated in malignant prostate lesions compared to benign prostate lesions (Muñoz et al. 2003). In agreement with these findings, we show Ki67 positive cells and thus proliferative activity in malignant tissue of the prostate tumours, while we detected only a limited number of proliferating cells in healthy prostate tissue (Fig. 14). In contrast to the tissue of origin, consistent with their growth in culture, organoids derived from the benign tissue contained cells positive for Ki67. Prostate tumour organoids also showed proliferative activity and from our observations in culture, there was a trend towards higher proliferation rate in the tumour organoids compared to the wildtype organoids.

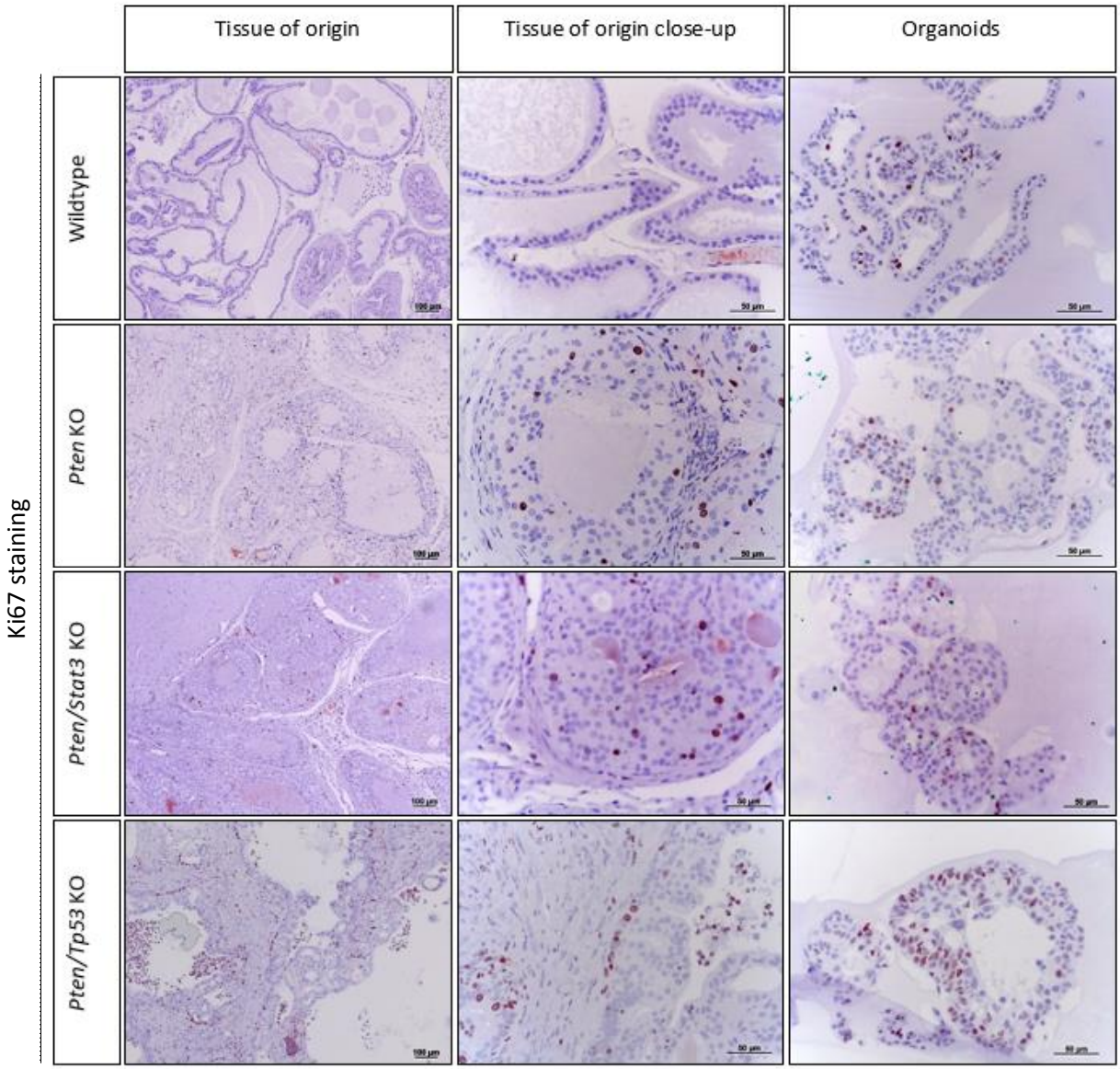

Figure 14

Comparison of murine Ki67 stained tissue of origin of *Pten, Pten/Stat3, Pten/Tp53* and wildtype tissue and organoids derived from the corresponding tissue. (Scale bars/Magnification: Tissue of origin ▬ 100 µm/10X; Tissue of origin close-up and Organoids ▬ 50 µm/20 and 40X.)

5.2.3 *STAT3 expression*

As the role of *Stat3* in PCa remains controversial, we stained the samples to assess the *STAT3* protein levels. We detected *STAT3* positive cells in all the tumour tissue and organoids except in *Pten/Stat3* knockouts and thus confirming the successful genetic deletion of *Stat3* in this mouse model. The wildtype tissue and organoids also possessed

Stat3 positive cells, although there was a trend towards *STAT3* upregulation in the tumour tissue and organoids (Fig. 15).

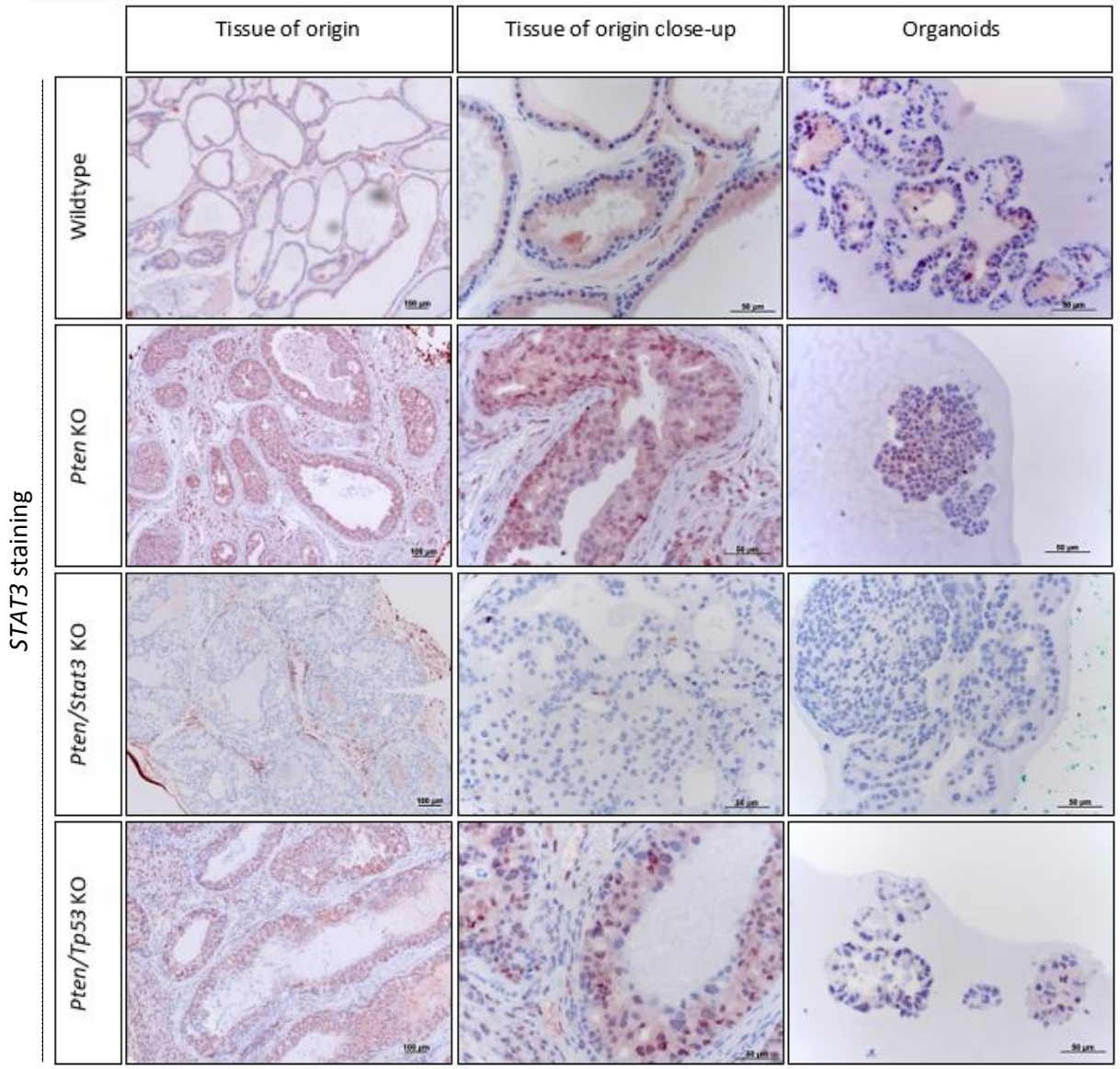

Figure 15
Comparison of murine *Stat3* stained tissue of origin of *Pten, Pten/Stat3, Pten/Tp53* and wildtype tissue and organoids derived from the corresponding tissue. (Scale bars/Magnification: Tissue of origin ▬ 100 µm/10X; Tissue of origin close-up and Organoids ▬ 50 µm/20 and 40X.)

5.2.4 pAKT expression

The AKT signalling pathway has been previously shown to be upregulated by loss of *Pten* (Song et al. 2012). Confirming this data, we observed increased pAKT staining in both tissue

of origin and organoids upon *Pten* loss and combination of *Pten/Stat3* and *Pten/Tp53* deletions. Neither wildtype tissue nor wildtype organoids showed cells expressing pAKT.

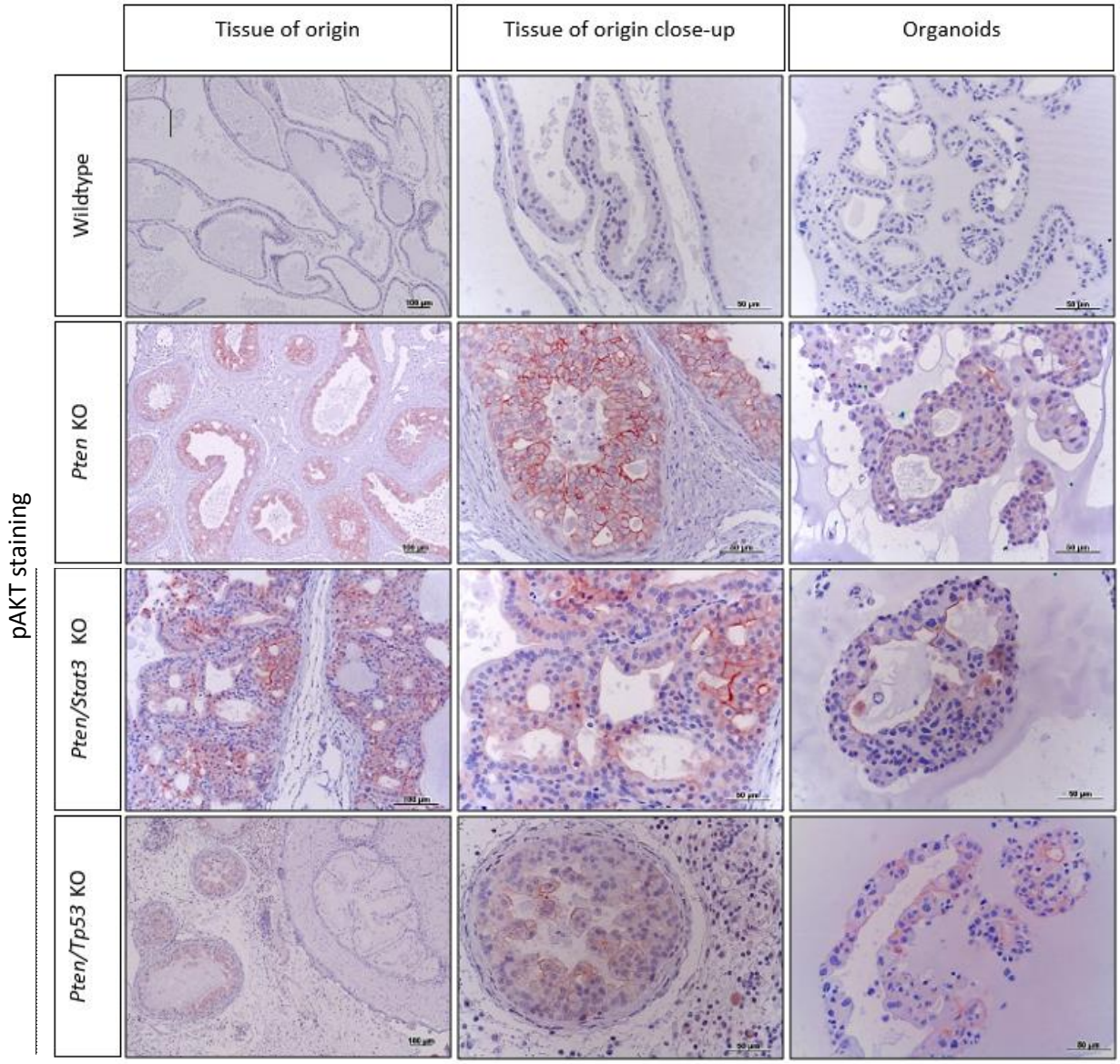

Figure 16
Comparison of murine pAKT stained tissue of origin of *Pten, Pten/Stat3, Pten/Tp53* and wildtype tissue and organoids derived from the corresponding tissue. (Scale bars/Magnification: Tissue of origin ▬ 100 µm/10X; Tissue of origin close-up and Organoids ▬ 50 µm/20 and 40X.)

5.2.5 Cytokeratin 8 (CK8) characterization

CK8 marks the luminal cells of the prostate. In a healthy prostate, these cells form an epithelial layer that surrounds the lumen into which they secrete prostatic proteins and fluids. It is indeed the luminal cells that in most cases of PCa undergo transformation and are responsible for the luminal phenotype of PCa (Zhang et al. 2018). In a healthy prostate

tissue and wildtype organoids, we detected the continuous epithelial luminal cell layer surrounding the lumen stained for CK8 (Fig.17). The CK8 staining in the benign prostate tissue was of reduced intensity and thus less visible due to technical limitations. As the healthy prostate gland structure is impaired in the tumour tissue and tumour organoids, also the CK8 staining differed to the benign tissue and organoids accordingly. In contrast to the wildtype tissue and organoids, CK8 positive cells in the tumour tissue and tumour organoids not only surrounded the tumour glands but were also present within the tumour tissue/organoids.

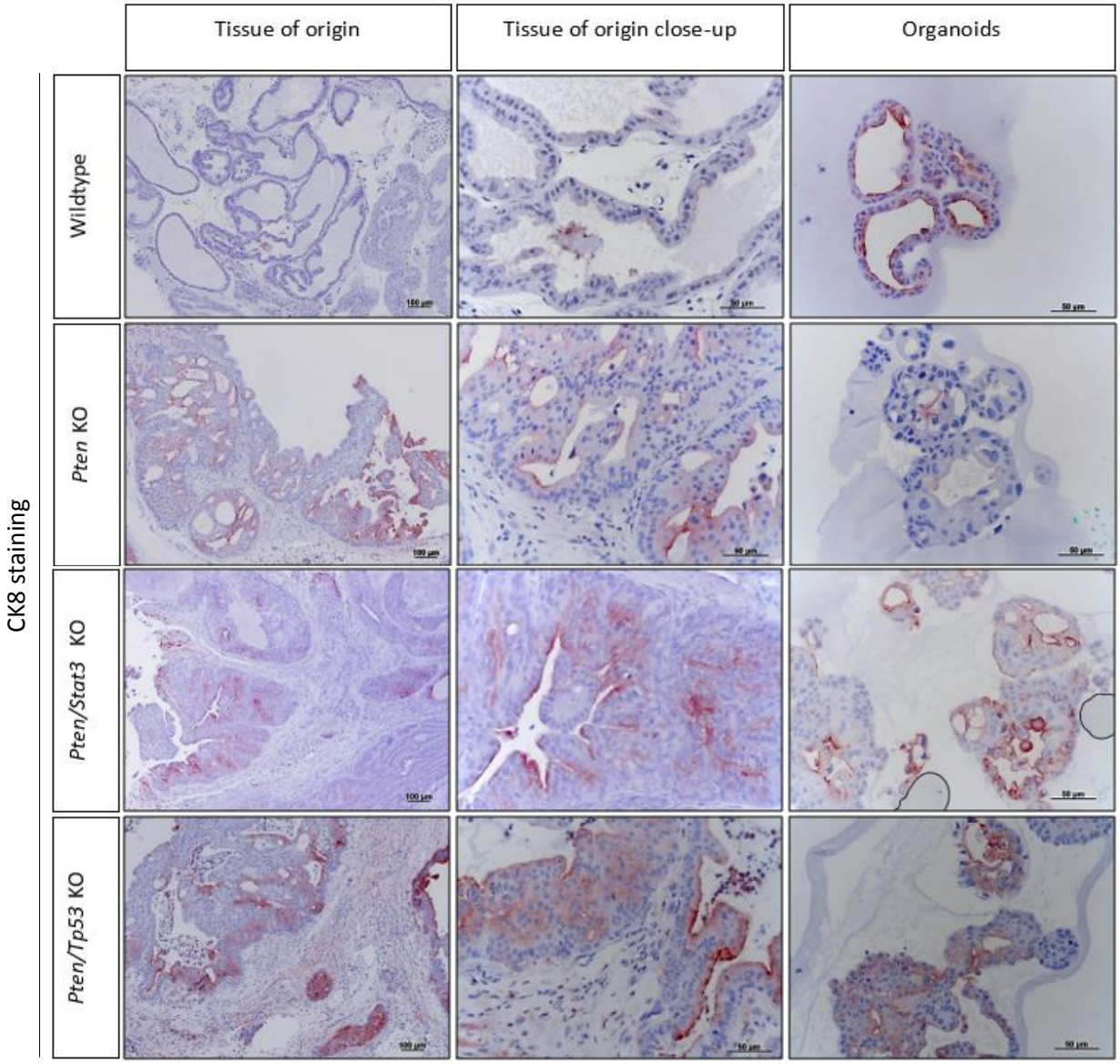

Figure 17

Comparison of murine CK stained tissue of origin of *Pten, Pten/Stat3, Pten/Tp53* and wildtype tissue and organoids derived from the corresponding tissue. (Scale bars/Magnification: Tissue of origin ▬ 100 µm/10X; Tissue of origin close-up and Organoids ▬ 50 µm/20 and 40X.)

5.3 Generating *in vitro* knockout of *Pten* and a double knockout of *Pten* and *Stat3* genes

5.3.1 ***In vitro Pten* knockout**

5.3.1.1 Lentiviral transduction of murine prostate organoids with MSCV CreERT2/CreCut puro plasmids

Wildtype murine prostate organoids with loxP sites flanking *Pten* gene were transduced with a tamoxifen (4HT) inducible Cre vector and a truncated, non-functional version of the Cre vector (CreCut) that was used as a control. After the transduction, samples were treated with puromycin for 2 weeks to ensure that only transduced organoids were selected. In order to verify the transduction success, DNA was isolated from both Cre and Crecut transduced organoids and genotyped with two different sets of primers confirming successful transduction (Fig. 18).

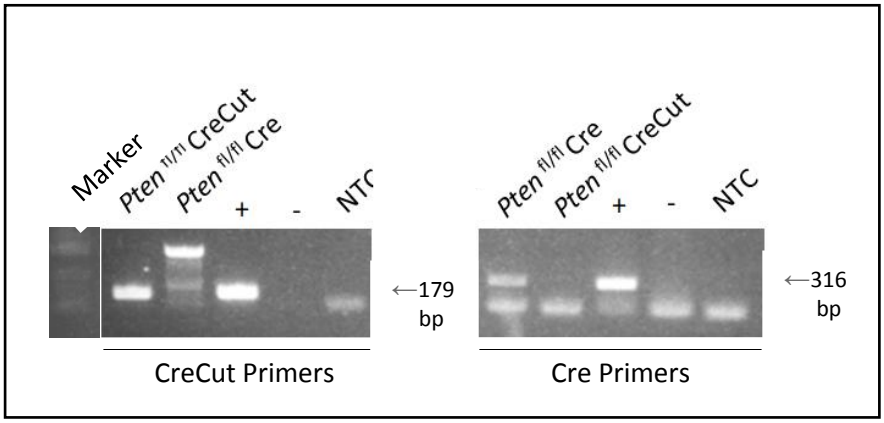

Figure 18
Genotyping of *Pten*$^{fl/fl}$ *Cre* and *Pten*$^{fl/fl}$ CreCut organoids. Cell lines containing the Cre and CreCut vector were used as a positive and negative controls. NTC = non template control.

5.3.1.2 Tamoxifen treatment of murine *Pten*$^{fl/fl}$ Cre and *Pten*$^{fl/fl}$ CreCut organoids

To induce the Cre vector and thus generate the *in vitro* knockout of *Pten*, the organoids were treated with 500nM 4HT for 4 weeks. They were monitored closely for any morphological changes. We detected higher proliferation rates in *Pten*$^{fl/fl}$ Cre organoids than in their control *Pten*$^{fl/fl}$ CreCut when plated at the same density as observed by microscopy (Fig 19).

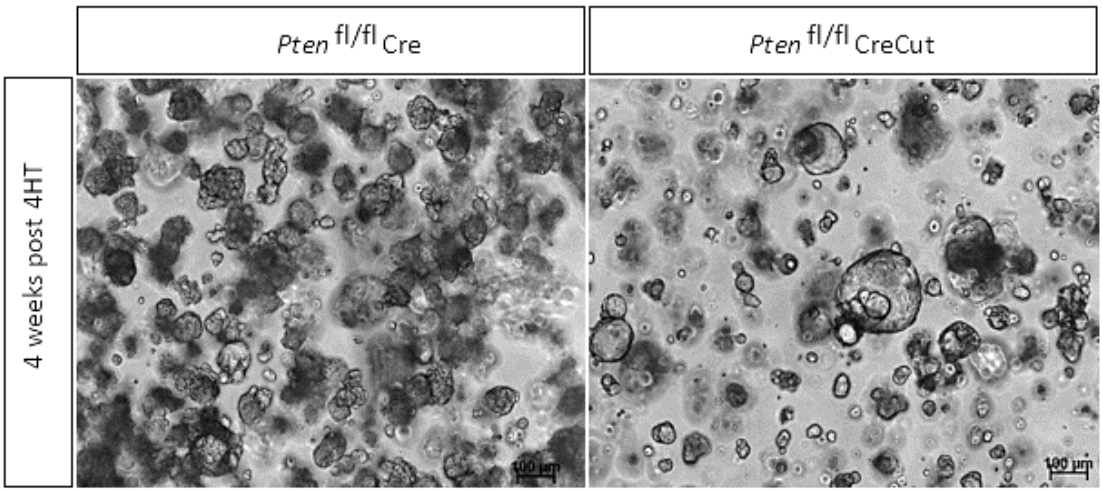

Figure 19
Bright field images of *Pten*$^{fl/fl}$ Cre and *Pten*$^{fl/fl}$ CreCut organoids. *Pten*$^{fl/fl}$ Cre organoids havehigher proliferative activity compared to the control. (Scale bar/Magnification: ▬ 100 µm/10X.)

5.3.1.3 Western blot analysis of murine *Pten*$^{fl/fl}$ Cre and *Pten*$^{fl/fl}$ CreCut organoids

Western blot analysis confirmed the successful generation of *in vitro Pten* knockouts in *Pten*$^{fl/fl}$ Cre organoids (Fig. 20). We did not detect any *Pten* protein 4 weeks post 4HT treatment in *Pten*$^{fl/fl}$ Cre organoids compared to the *Pten*$^{fl/fl}$ CreCut control. The tumour tissue of a *Pten* KO mouse that was used as a knockout control showed a reduced *Pten* expression but not a full knockout. The *Pten* function in this mouse model was disturbed by deleting exon 5. The protein is non-functional, but the first exons are still recognized by the PTEN antibody. Expression levels of pAKT are upregulated in *Pten*$^{fl/fl}$ Cre organoids. In contrast, pAKT protein is not detectable in *Pten*$^{fl/fl}$ CreCut organoids. There are no differences in pSTAT3 levels amongst the samples.

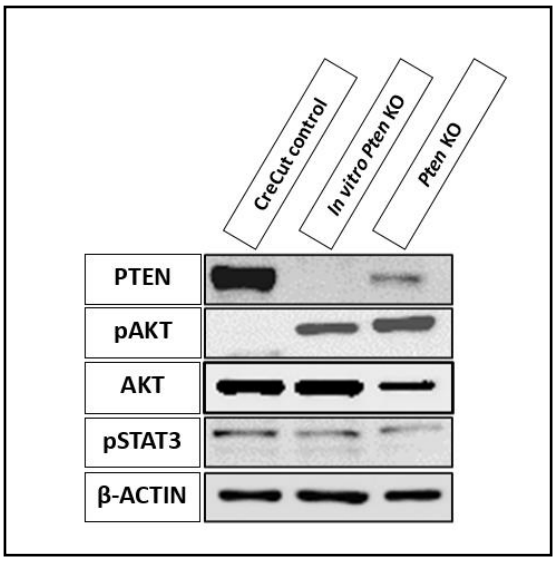

Figure 20
Western blot analysis of *Pten*$^{fl/fl}$ Cre and *Pten*$^{fl/fl}$ CreCut organoids. A *Pten* KO tumour tissue was used as a control.

5.3.1.4 Characterization of murine *in vitro Pten* knockout organoids by HE and IHC staining

To further characterize the *in vitro Pten* knockout organoids, they were embedded and analyzed by HE and Ki67 IHC staining. We observed histological differences between the HE stained knockout organoids and the control as seen in Figure 21. While the majority of wildtype organoids had a ductal structure with bi-layered epithelium surrounding a lumen resembling a healthy prostate gland, deletion of *Pten* resulted in organoids that possessed multiple inner layers and mostly no prostate lumen. This phenotype resembled the PCa phenotype seen *in vivo.*

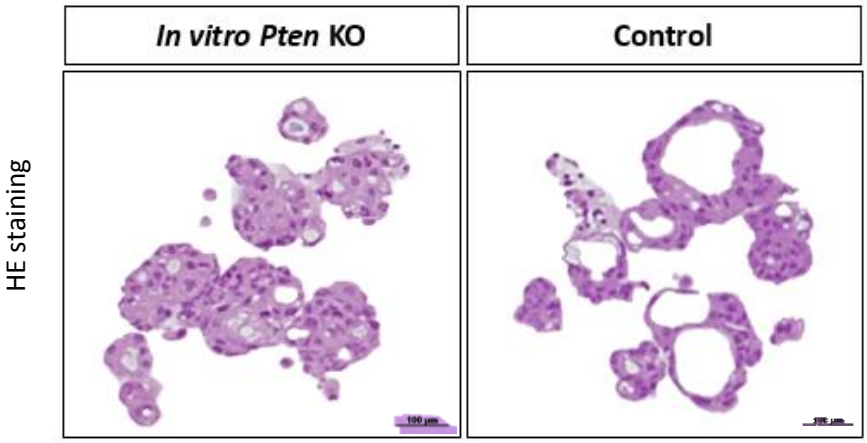

Figure 21
Comparison of HE stained *in vitro Pten* KO organoids and their control. (Scale bar/Magnification: ▬ 100 µm/20X.)

The Ki67 staining showed active proliferation in both *in vitro Pten* knockout organoids and the control consistent with their growth in culture.

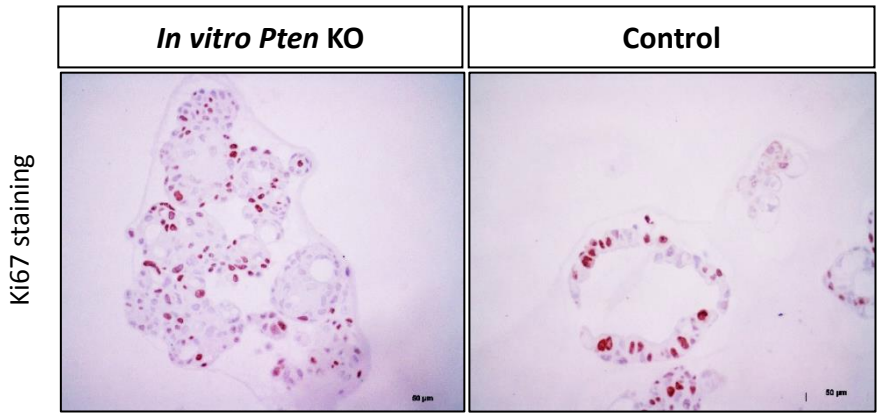

Figure 22
Comparison of Ki67 stained *in vitro Pten* KO organoids and their control. (Scale bar/Magnification: ▬ 100 µm/20X.)

5.3.1.5 Proliferation assay of *in vitro Pten* knockout organoids

To assess the proliferation rate of the *in vitro Pten* knockout organoids, we performed Resazurin proliferation assay. As the graph indicates, *in vitro Pten* knockout organoids showed higher proliferative activity compared to the control, which confirmed our observations in culture. Nevertheless, due to high varience within the samples the difference in proliferation was not statistically significant.

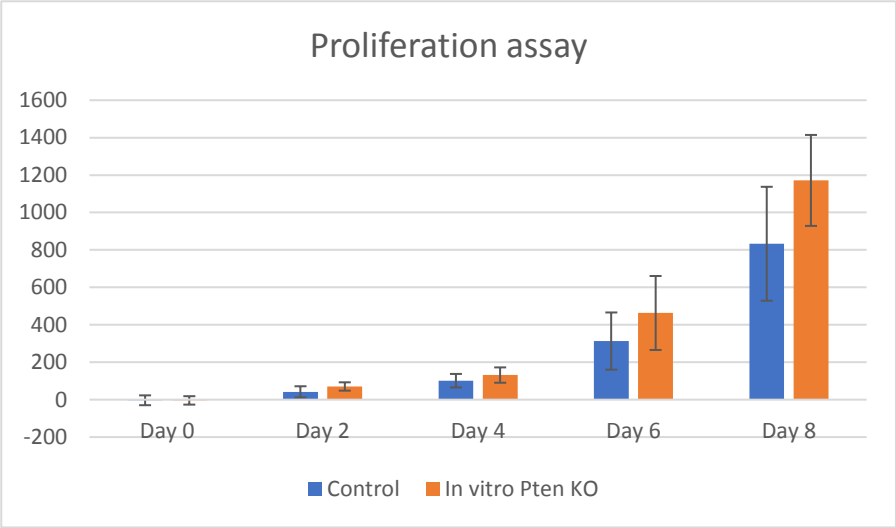

Figure 23
Proliferation rate of *in vitro Pten* KO organoids and their control. 7000 cells/Matrigel were seeded and measured on day 0, 2, 4, 6 and 8.

5.3.2 *In vitro* Pten/Stat3 knockout

5.3.2.1 Electroporation of murine prostate organoids with MSCV CreERT2/CreCut puro plasmid

Wildtype murine prostate organoids with loxP sites flanking the *Pten* and *Stat3* gene were electroporated with the already above mentioned Cre and Crecut vector. Similarly, as with the generation of in *vitro Pten* knockout, samples were treated with puromycin for 2 weeks after the electroporation and genotyped with Cre and CreCut primers. Both Cre and CreCut bands resemble their control bands thus the transduction was successful.

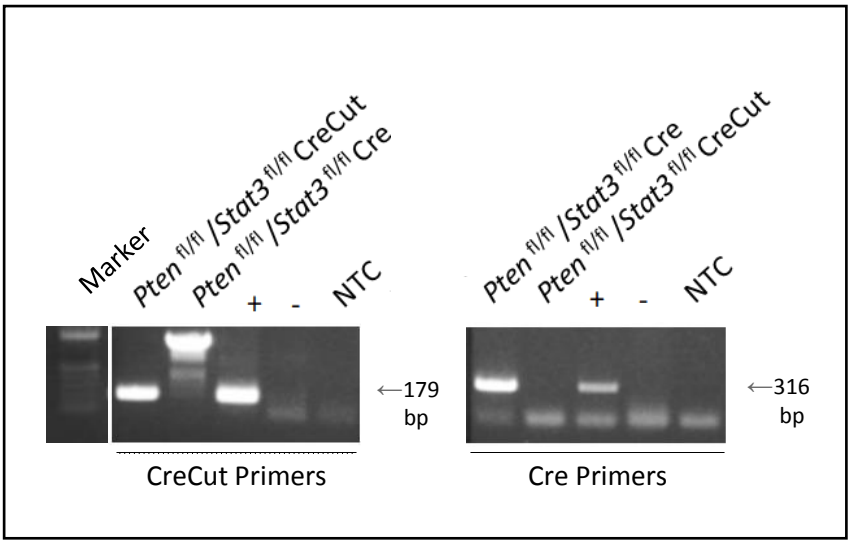

Figure 24
Genotyped DNA samples of *Pten*$^{fl/fl}$/*Stat3*$^{fl/fl}$ Cre and *Pten*$^{fl/fl}$/*Stat3*$^{fl/fl}$ CreCut organoids. Cell lines containing the Cre and CreCut vector were used as a positive and negative controls. NTC = non template control.

5.3.2.2 Tamoxifen treatment of murine *Pten*$^{fl/fl}$/*Stat3*$^{fl/fl}$ and *Pten*$^{fl/fl}$/*Stat3*$^{fl/fl}$ CreCut organoids

The organoids were further treated with 500nM 4HT and monitored closely for any morphological changes. Such changes could be seen already two weeks post 4HT treatment. While the control organoids were mostly of a round shape and cystic, the majority of *Pten*$^{fl/fl}$/*Stat3*$^{fl/fl}$ Cre organoids grew bigger and showed a dense morphology partially accompanied by irregular budding structures.

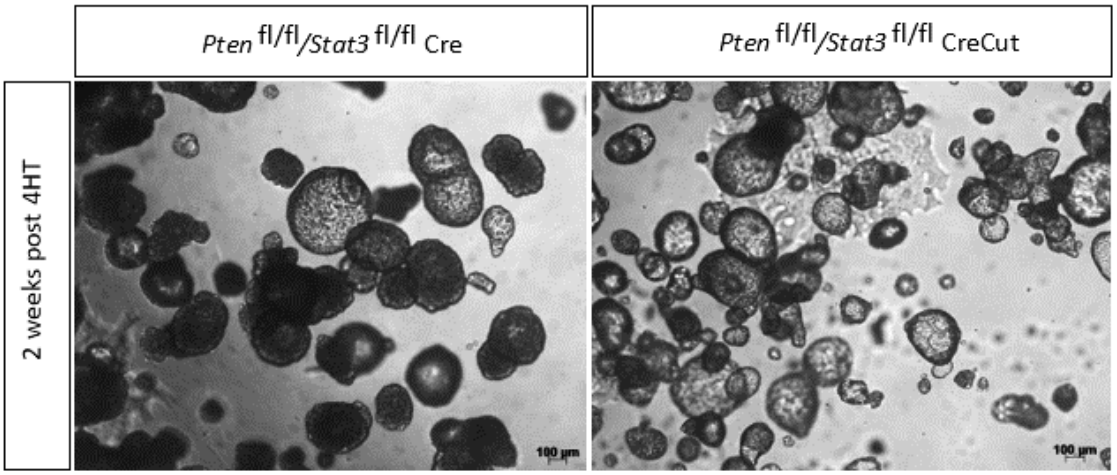

Figure 25
Bright field images of *Pten*$^{fl/fl}$/*Stat3*$^{fl/fl}$ Cre and *Pten*$^{fl/fl}$/*Stat3*$^{fl/fl}$ CreCut organoids indicating morphological differences between the genotypes. (Scale bar/Magnification: 100 µm/5X.)

5.3.2.3 Western blot analysis of murine *Pten*$^{fl/fl}$/*Stat3*$^{fl/fl}$ Cre and *Pten*$^{fl/fl}$/*Stat3*$^{fl/fl}$ CreCut organoids

To confirm the successful deletion of *Pten* and *Stat3*, proteins were isolated one and two weeks post 4HT treatment and analyzed via western blot analysis (Fig. 30). While *Stat3* deletion was evident already in one-week 4HT treated organoids, *Pten* protein levels were reduced upon one week of 4HT treatment and the full knockout of *Pten* was complete in two-weeks 4HT treated organoids. A *Pten/Stat3* KO tumour tissue was used as a knockout control. Both *Pten* and *Stat3* protein levels did not change in the CreCut organoid controls as well as in untreated Cre and CreCut samples. Similarly, as in the *in vitro Pten* knockout, pAKT protein levels were elevated upon *Pten* loss.

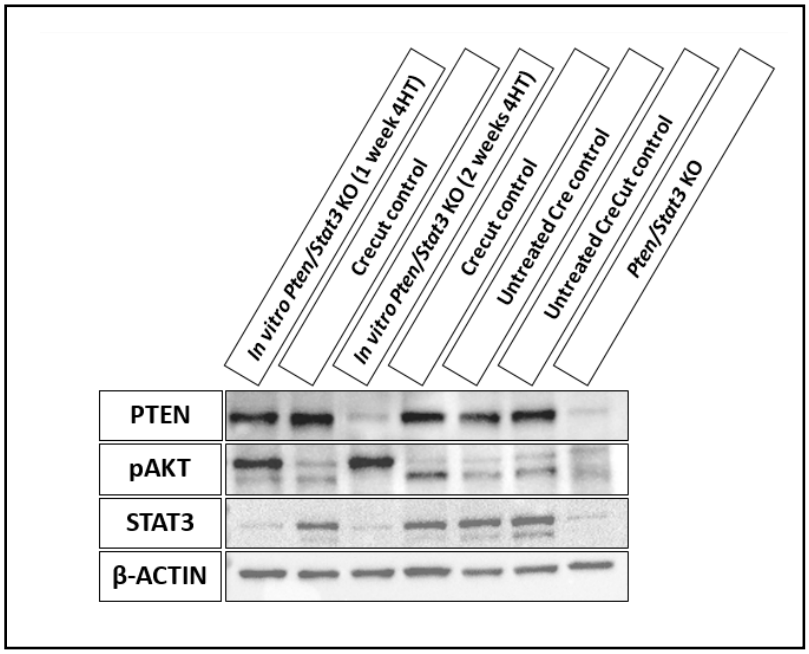

Figure 26
Western blot analysis of *Pten*$^{fl/fl}$/*Stat3*$^{fl/fl}$ and *Pten*$^{fl/fl}$/*Stat3*$^{fl/fl}$ CreCut organoids. *Pten/Stat3* KO tumour tissue was used as a knocknout control.

5.3.2.4 Characterization of murine *in vitro Pten/Stat3* knockout organoids by HE and IF staining

Embedded and HE stained organoids possessed histological differences between *in vitro Pten/Stat3* knockout and the control as seen on Figure 27. Similarly, as the *in vitro Pten* knockout organoids, also *Pten/Stat3* knockout organoids showed multiple inner epithelial

layers in contrast to bi- and single-layered epithelium of control organoids and resemble the PCa phenotype seen *in vivo.*

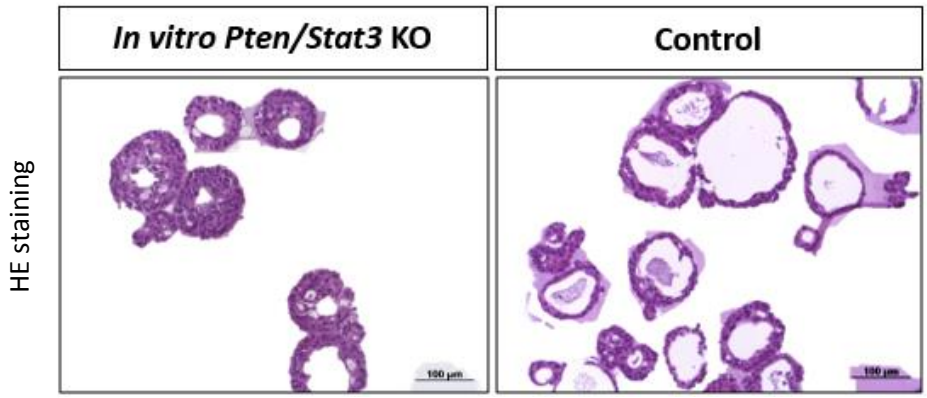

Figure 27
Comparison of HE stained *in vitro Pten/Stat3* KO organoids and their control indicated histological differences between the samples. (Scale bar/Magnification: ▬ 100 µm/20X.)

The Ki67 staining showed active proliferation in both organoid cultures (Fig. 28). Cells with basal origin were stained by CK14. The wildtype organoids showed organized structures that resembled a basal cell layer, whereas in the knockout organoids these cells were randomly distributed within the organoid.

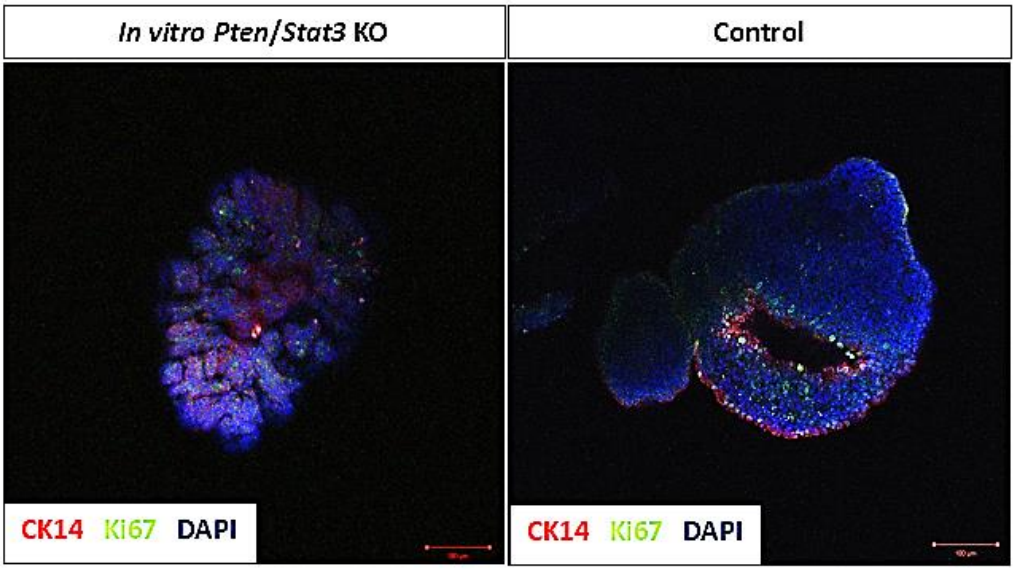

Figure 28
Comparison of *in vitro Pten/Stat3* KO organoids and their control stained by IF. The CK14 positive cells are displayed in red, Ki67 positive cells in green and DAPI positive cells in blue. (Scale bar/Magnification: ▬ 100 µm/25X.)

5.3.2.5 Proliferation assay of murine *in vitro Pten/Stat3* knockout organoids

To quantify the proliferation rate of the *in vitro Pten/Stat3* knockout organoids in different seeding densities, Resazurin proliferation assays were performed (Figs. 29, 30). According to our results, *in vitro Pten/Stat3* knockout organoids had slightly higher proliferative activity (except on day 6) compared to their control when plated both in low and high density. The measurements from day 6 indicated that control organoids proliferated significantly more than *in vitro Pten/Stat3* knockout organoids on this day in both seeding situations. Overall, both control and the *in vitro Pten/Stat3* knockout organoids had higher proliferative activity when seeded in lower seeding density.

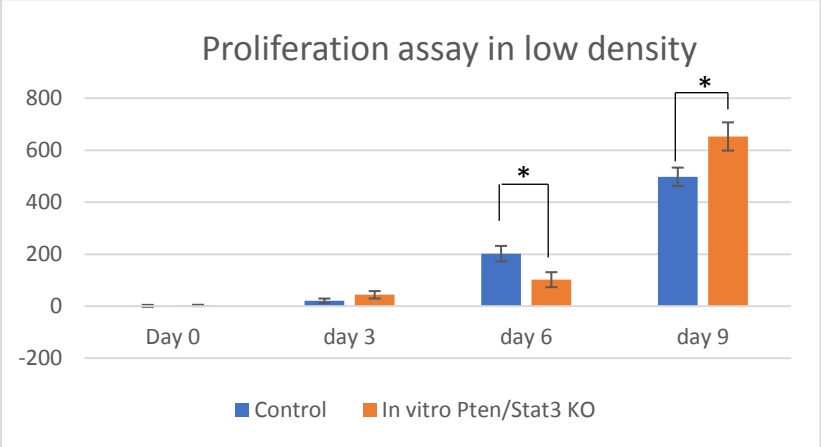

Figure 29
Proliferation rate of *in vitro Pten/Stat3* KO organoids and their control. 3500 cells/Matrigel were seeded and measured at day 0, 3, 6 and 9. The difference in proliferation on day 6 and 9 between samples was statistically significant (*p < 0.05, two-tailed Student's t-test).

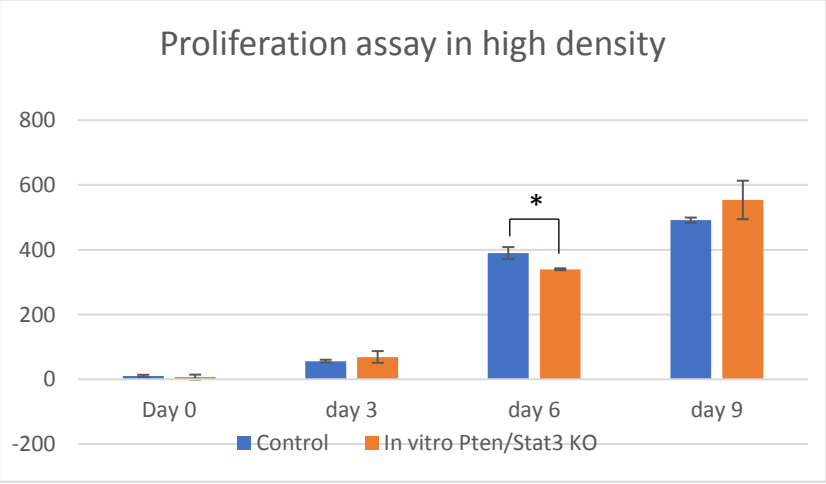

Figure 30
Proliferation rate of *in vitro Pten/Stat3* KO organoids and their control. 7000 cells/Matrigel were seeded and measured at day 0, 3, 6 and 9. The difference in proliferation on day 6 between samples was statistically significant (*p <0.05, two-tailed Student's t-test).

6 Discussion

6.1 Characterization of murine prostate organoids of different genetic background

We established a panel of benign and malignant organoid lines derived from different genetic backgrounds and characterized them in biological triplicates for their histo-morphology, protein expression and proliferation. All tumour organoid lines derived from a single knockout of *Pten* or double knockouts of *Pten/Stat3* and *Pten/Tp53* deficient mice morphologically reflected the tissue of origin and resembled phenotypes seen in human PCa. The wildtype organoids mimicked the healthy prostate glands.

Our results show active proliferation in the tumour organoids as well as in the wildtype organoids via Ki67 staining. Even though the healthy prostate tissue does not possess many Ki67 positive cells, the active proliferation in the wildtype organoids was supported by the culture conditions. The culture medium contains different growth factors, vitamins and other components that promote proliferation of epithelial cells, both healthy and cancerous. For instance Epidermal growth factor (EGF) was shown to promote dimerization of its receptor EGFR (Kovacs et al. 2015) which further led to upregulation of signalling pathways such as PI3K/AKT which is known to effect cell proliferation (Vivanco and Sawyers 2002) and was described in earlier chapters in context of *PTEN* loss. This effect is therefore enhanced in our knockout organoids but is eventually blocked by the downstream effectors such as *PTEN* in the wildtype organoids. Hence, we see pAKT upregulation in *Pten* deficient organoids but not in the wildtype organoids. The literature describes mitogenic effects of EGF amongst epidermal and epithelial cells, glial cells, vascular cells, mammary epithelial cells and others (Schlessinger et al. 1983). This growth factor is isolated from the submaxillary glands of adult male mice or from human urine and is used to promote proliferation in cell culture media (Cohen and Carpenter 1975).

Consistent with the literature and our data from established *in vitro* knockouts, tumour organoids as well as their tissue of origin had upregulated pAKT signalling, whereas wildtype tissue and organoids did not show any pAKT positive cells. Also, the CK8 staining of the organoids marking the luminal cells mimicked the tissue of origin. Although, the CK8 staining of the healthy tissue was difficult to detect due to technical limitations. A longer

incubation time with AEC chromogen should be performed in order to enhance the staining intensity.

Based on this data, we can conclude that the murine organoid cultures serve as a great alternative model system to study human PCa. Both malignant and benign organoids grow easily in culture for many passages, they reflect the tissue of origin histologically as well as considering the signalling responses as seen *in vivo*. However, further characterization of this model with additional IHC stainings should be considered.

For instance, p63 staining of basal cells is routinely used in diagnostics of PCa (Weinstein et al. 2002) as the loss of basal cells belongs to one of the most important hallmarks of malignancy (Humphrey 2012). Such staining was done by Karthaus et al. who demonstrated healthy prostate murine organoids forming continuous basal cell layer expressing exclusively basal prostate markers (Karthaus et al. 2014). We would expect similar findings in our wildtype organoids. Based on the changes we observed in the CK8 stained luminal cells, we speculate that the outer basal cell layer in tumour organoids and tissue will most certainly be impaired.

As cancer is traditionally associated with many molecular abnormalities such as chromosomal instability, gene mutations and double-strand breaks (DSB), gamma-H2AX staining as a mark of DSB (Kuo and Yang 2008) would allow us to assess such damage in our murine organoid cultures and the tissue of origin. DSBs are repaired by cellular DNA damage repair (DDR) systems that prevent tumorigenesis (Jackson and Bartek 2009). Amongst the DDR proteins is the ATM protein which was shown to have a tumour suppressive function (Shiloh 2003). Activation of both DSB and ATM were observed in pre-cancerous lesions (Gorgoulis et al. 2005). Recently, a novel mechanism of spontaneous DSB (spDSB) in cancer cells was described by activation of apoptotic caspases and nucleases. Instead of causing apoptosis as previously described, the spDSB were shown to drive tumorigenesis and stemness of cancer cells through activation of DDR proteins such as ATM or ATR (Liu et al. 2017). Staining for DSBs could elaborate on the effect of different knockouts on the DNA damage.

Cleaved caspase 3 (CC3), a cell death protease, is activated during apoptosis and serves as an apoptotic marker. Although, recent evidence suggests other non-apoptotic roles of this protein. Surprisingly, upregulated levels of CC3 were shown to correlate with progression of four cancer types – gastric, ovarian, cervical and colorectal cancers – and its pathological

risk factors such as for instance tumour stage or lymph-node metastasis in those cancer entities (Hu et al. 2014). Huang et al. examined the unexpected mechanism of growth stimulation by CC3 in dying tumour cells after undergoing radiotherapy and demonstrated that CC3 promotes release of growth signals such as calcium independent phospholipase A_2 ($iPLA_2$) that leads to tumour repopulation (Huang et al. 2011). These findings indicate that CC3 has a prognostic potential and based on this data, we would expect elevated CC3 staining in our murine tumour organoids and tissue.

Also p21, an oncogene in some cancer types and a tumour suppressor in others (Abbas and Dutta 2009), was shown to induce apoptosis and reduce tumour size in PCa in mice upon p21 over-expression (Eastham et al. 1995) while in another study, loss of p21 led to protection against tumorigenesis in the prostate (Jain et al. 2013). The cyclin-dependent kinase inhibitors (CDKI) such as p21 regulate the progression through the cell cycle (Wade Harper 1993). Moreover, p21 activity has been associated with p53 status, which activates p21 upon DNA damage and thereby negatively regulates the cell cycle (Vermeulen et al. 2003). Although other p53-independent induction pathways of p21 were reported (Datto et al. 1995), it would be interesting to see the p21 status in our samples.

These additional IHC stainings would help us further characterize this model system and potentially shed light on some of the controversial hypotheses regarding the signalling pathways.

The next stage of our organoid models would also be establishing these organoids in co-culture with other cellular components of the tumour, for instance stromal cells. The stromal compartment of the prostate consists of different growth factors, chemokines, cytokines, extracellular matrix (ECM) and various cell types such as fibroblasts, myofibroblasts, endothelial cells and immune cells (Josson et al. 2010). The tumour microenvironment is recognized as an important player in development and progression of cancer. There are several known mechanisms that lead to tumour progression caused by the crosstalk between prostate epithelial cells and the stromal compartment. Such crosstalk in signalling can result in ECM remodelling, which further promotes invasion, stimulation of angiogenesis and release of growth factors (Tuxhorn et al. 2001). Stromal cells were shown to develop genetic alterations when in close proximity to the tumour (Hill et al. 2005). While the healthy prostate surrounded by mainly smooth muscle cells depends on the signals from these stromal cells to sustain organ homeostasis, the altered

phenotype of these cells in PCa leads to promoting the tumour progression (Cunha et al. 1996). For instance, healthy fibroblasts help to synthesize the ECM (Rodemann and Müller 1991), they form the basement membrane, which separates the epithelium from the stroma (Chang et al. 2002) and were shown to become activated during wound healing to generate the ECM for tissue regeneration (Tomasek et al. 2002). In contrast, cancer associated fibroblasts (CAF) are constantly activated and secrete growth factors and chemokines that promote additional oncogenic signals leading to cancer cell proliferation and invasion (Liotta and Kohn 2001). CAFs were demonstrated to be the most abundant cell type in the tumour stroma (Liotta and Kohn 2001).

In 2018, co-cultures of primary pancreatic cancer organoids together with the stromal and immune components from the pancreatic tumour were already established (Tsai et al. 2018) and culturing the PCa organoids with the stromal and immune cells would increase the accuracy of this model as a preclinical cancer model.

6.2 *In vitro* knockouts

In this study, we show a successful generation of *in vitro Pten* and *Pten/Stat3* knockouts in wildtype murine prostate organoids via the Cre-lox recombination system. Tamoxifen inducible Cre vectors were delivered into the organoids through lentiviral transduction or electroporation with the NEPA21 electroporator. We conclude that both methods are suitable to transfect murine prostate organoids.

We confirmed the successful generation of the *in vitro* knockouts with western blot analysis.

While the proteins of *Pten*$^{fl/fl}$ Cre/Crecut organoids were first isolated upon 4 weeks of tamoxifen treatment, *Pten*$^{fl/fl}$/*Stat3*$^{fl/fl}$ Cre/Crecut samples were analyzed for the deletions already upon 1 and 2 weeks of tamoxifen treatment due to a larger sample size and thus available protein. We show a complete loss of *Stat3* upon 1 week of treatment, whereas the expression of *Pten* is only reduced upon 1 week of treatment and fully lost in 2-weeks treated *Pten*$^{fl/fl}$/*Stat3*$^{fl/fl}$ Cre organoids. The efficiency of tamoxifen inducible Cre-lox recombination might vary depending on the dose and duration of tamoxifen treatment, the levels of Cre recombinase expression and the accessibility of the floxed alleles based on their chromatin structure and epigenetic status (Buelow and Scharenberg 2008; Long

and Rossi 2009; Guo et al. 2002). The different gene loci might therefore have different optimal tamoxifen treatment conditions. We demonstrate that already reduced expression of *Pten* results in upregulation of the pAKT signalling pathway.

Our data further show that Cre-driven excision of *Pten* and Pten/Stat3 *in vitro* leads to organoids that resemble PCa phenotypes. The organoids of both *in vitro* knockouts form multiple layers of epithelium with structures that mimic the features of prostate tumours and the budding structure of those organoids protruding into Matrigel suggests invasive behaviour as seen in the tumour organoids. With these findings we confirm the hypothesis of Pencik et. al and hence the tumour suppressive function of *Stat3* in *Pten* deficient model (Pencik et al. 2015a). The knockout organoids also show higher proliferative activity measured over time with the Resazurin proliferation assay as well as via our observations in culture. We assume that the difference in proliferation on day 6 between the *in vitro* Pten/Stat3 knockout organoids and the control organoids are due to higher metabolism of the *in vitro* knockout organoids and thus earlier use-up of the medium components prior to the medium exchange. As a consequence, the *in vitro* knockout organoids grow faster initially to a certain size and then slow down the growth upon medium usage. The continuous growth is then restored after medium exchange as seen on day 9. In contrast, the control organoids grow with the same rate over time. Our results also indicate that both control and *in vitro Pten/Stat3* knockout organoids tend to proliferate more in lower seeding density. When the cells are plated too dense, it might lead to contact inhibition that slows down the growth of the organoids. In contrast, from our observations in culture, very low seeding density (less than 50 cells in 6 µl Matrigel) also effects the growth towards slower proliferation. This indicates that optimal seeding density and signalling between cells is essential for their growth.

We propose the presented *in vitro* knockouts of PCa relevant genes as a new valid organoid model to analyze the processes of malignant transformation. Such model has been introduced in two independent studies, in which upon introduction of oncogenic mutations by CRISPR/Cas9 in colon organoids resulted in phenotypes observed in colon cancer patients (Drost et al. 2015; Matano et al. 2015).

CRISPR/Cas9 as a novel genome editing technique allows disruption or repair of any desired gene with high specificity. It was first used in organoids in 2013, when Schwank et. al demonstrated as the proof of concept the repair of the CFTR gene with help of

CRISPR/Cas9 in intestinal stem cell organoids of cystic fibrosis patients (Schwank et al. 2013). The genome editing with CRISPR/Cas9 technology eliminates the need of genetically engineered mouse and in combination with organoid technology would allow us to create a biobank of organoid lines harbouring different PCa relevant mutations. Such biobanks could be used to study tumorigenesis and the signalling pathways upon which the malignant transformation occurs and would also have large applications in high throughput screening to discover new drug therapies, test different drug combinations or drug resistance.

7 Publication bibliography

Abbas, Tarek; Dutta, Anindya (2009): p21 in cancer: intricate networks and multiple activities. In *Nature reviews. Cancer* 9 (6), pp. 400–414. DOI: 10.1038/nrc2657.

Abdulghani, Junaid; Gu, Lei; Dagvadorj, Ayush; Lutz, Jacqueline; Leiby, Benjamin; Bonuccelli, Gloria et al. (2008): Stat3 promotes metastatic progression of prostate cancer. In *The American journal of pathology* 172 (6), pp. 1717–1728. DOI: 10.2353/ajpath.2008.071054.

Aumüller, G. (1979): Seminal Vesicles. In A. Oksche, L. Vollrath, G. Aumüller (Eds.): Prostate Gland and Seminal Vesicles, 7 / 6. Berlin, Heidelberg: Springer Berlin Heidelberg (Handbuch der mikroskopischen Anatomie des Menschen), pp. 183–267.

Baker, S. J.; Fearon, E. R.; Nigro, J. M.; Hamilton, S. R.; Preisinger, A. C.; Jessup, J. M. et al. (1989): Chromosome 17 deletions and p53 gene mutations in colorectal carcinomas. In *Science (New York, N.Y.)* 244 (4901), pp. 217–221. DOI: 10.1126/science.2649981.

Barbieri, Christopher E.; Baca, Sylvan C.; Lawrence, Michael S.; Demichelis, Francesca; Blattner, Mirjam; Theurillat, Jean-Philippe et al. (2012): Exome sequencing identifies recurrent SPOP, FOXA1 and MED12 mutations in prostate cancer. In *Nature genetics* 44 (6), pp. 685–689. DOI: 10.1038/ng.2279.

Bates, S.; Phillips, A. C.; Clark, P. A.; Stott, F.; Peters, G.; Ludwig, R. L.; Vousden, K. H. (1998): p14ARF links the tumour suppressors RB and p53. In *Nature* 395 (6698), pp. 124–125. DOI: 10.1038/25867.

Berger, Michael F.; Lawrence, Michael S.; Demichelis, Francesca; Drier, Yotam; Cibulskis, Kristian; Sivachenko, Andrey Y. et al. (2011): The genomic complexity of primary human prostate cancer. In *Nature* 470 (7333), pp. 214–220. DOI: 10.1038/nature09744.

Berquin, Isabelle M.; Min, Younong; Wu, Ruping; Wu, Hong; Chen, Yong Q. (2005): Expression signature of the mouse prostate. In *The Journal of biological chemistry* 280 (43), pp. 36442–36451. DOI: 10.1074/jbc.M504945200.

Bray, Freddie; Ferlay, Jacques; Soerjomataram, Isabelle; Siegel, Rebecca L.; Torre, Lindsey A.; Jemal, Ahmedin (2018): Global cancer statistics 2018: GLOBOCAN estimates of incidence and mortality worldwide for 36 cancers in 185 countries. In *CA: a cancer journal for clinicians* 68 (6), pp. 394–424. DOI: 10.3322/caac.21492.

Brinkmann, A. O.; Kuiper, G.G.J.M.; Ris-Stalpers, C.; van Rooij, H.C.J.; Romalo, G.; Trifiro, M. et al. (1991): Androgen receptor abnormalities. In *The Journal of Steroid Biochemistry and Molecular Biology* 40 (1-3), pp. 349–352. DOI: 10.1016/0960-0760(91)90201-f.

Buelow, Ben; Scharenberg, Andrew M. (2008): Characterization of parameters required for effective use of tamoxifen-regulated recombination. In *PloS one* 3 (9), e3264. DOI: 10.1371/journal.pone.0003264.

Buttyan, R.; Sawczuk, I. S.; Benson, M. C.; Siegal, J. D.; Olsson, C. A. (1987): Enhanced expression of the c-myc protooncogene in high-grade human prostate cancers. In *The Prostate* 11 (4), pp. 327–337. DOI: 10.1002/pros.2990110405.

Chen, Zhenbang; Trotman, Lloyd C.; Shaffer, David; Lin, Hui-Kuan; Dotan, Zohar A.; Niki, Masaru et al. (2005): Crucial role of p53-dependent cellular senescence in suppression of Pten-deficient tumorigenesis. In *Nature* 436 (7051), pp. 725–730. DOI: 10.1038/nature03918.

Chua, Chee Wai; Shibata, Maho; Lei, Ming; Toivanen, Roxanne; Barlow, LaMont J.; Bergren, Sarah K. et al. (2014): Single luminal epithelial progenitors can generate prostate organoids in culture. In *Nature cell biology* 16 (10), 951-61, 1-4. DOI: 10.1038/ncb3047.

Cohen, S.; Carpenter, G. (1975): Human epidermal growth factor: isolation and chemical and biological properties. In *Proceedings of the National Academy of Sciences of the United States of America* 72 (4), pp. 1317–1321. DOI: 10.1073/pnas.72.4.1317.

Culig, Zoran (2014): Distinguishing indolent from aggressive prostate cancer. In *Recent results in cancer research. Fortschritte der Krebsforschung. Progres dans les recherches sur le cancer* 202, pp. 141–147. DOI: 10.1007/978-3-642-45195-9_17.

Cunha, G. R.; Donjacour, A. A.; Cooke, P. S.; Mee, S.; Bigsby, R. M.; Higgins, S. J.; Sugimura, Y. (1987): The endocrinology and developmental biology of the prostate. In *Endocrine reviews* 8 (3), pp. 338–362. DOI: 10.1210/edrv-8-3-338.

Cunha, G. R.; Hayward, S. W.; Dahiya, R.; Foster, B. A. (1996): Smooth muscle-epithelial interactions in normal and neoplastic prostatic development. In *Acta anatomica* 155 (1), pp. 63–72. DOI: 10.1159/000147791.

Cunningham, David; You, Zongbing (2015): In vitro and in vivo model systems used in prostate cancer research. In *Journal of biological methods* 2 (1). DOI: 10.14440/jbm.2015.63.

Cybulski, Cezary; Huzarski, Tomasz; Górski, Bohdan; Masojć, Bartłomiej; Mierzejewski, Marek; Debniak, Tadeusz et al. (2004): A novel founder CHEK2 mutation is associated with increased prostate cancer risk. In *Cancer Res* 64 (8), pp. 2677–2679. DOI: 10.1158/0008-5472.CAN-04-0341.

Datto, M. B.; Li, Y.; Panus, J. F.; Howe, D. J.; Xiong, Y.; Wang, X. F. (1995): Transforming growth factor beta induces the cyclin-dependent kinase inhibitor p21 through a p53-independent mechanism. In *Proceedings of the National Academy of Sciences of the United States of America* 92 (12), pp. 5545–5549. DOI: 10.1073/pnas.92.12.5545.

Dauer, Daniel J.; Ferraro, Bernadette; Song, Lanxi; Yu, Bin; Mora, Linda; Buettner, Ralf et al. (2005): Stat3 regulates genes common to both wound healing and cancer. In *Oncogene* 24 (21), pp. 3397–3408. DOI: 10.1038/sj.onc.1208469.

Donehower, L. A.; Harvey, M.; Slagle, B. L.; McArthur, M. J.; Montgomery, C. A.; Butel, J. S.; Bradley, A. (1992): Mice deficient for p53 are developmentally normal but susceptible to spontaneous tumours. In *Nature* 356 (6366), pp. 215–221. DOI: 10.1038/356215a0.

Donjacour, Annemarie A.; Cunha, Gerald R. (1988): The effect of androgen deprivation on branching morphogenesis in the mouse prostate. In *Developmental Biology* 128 (1), pp. 1–14. DOI: 10.1016/0012-1606(88)90260-6.

Draisma, Gerrit; Etzioni, Ruth; Tsodikov, Alex; Mariotto, Angela; Wever, Elisabeth; Gulati, Roman et al. (2009): Lead time and overdiagnosis in prostate-specific antigen screening: importance of methods and context. In *Journal of the National Cancer Institute* 101 (6), pp. 374–383. DOI: 10.1093/jnci/djp001.

Drost, Jarno; Karthaus, Wouter R.; Gao, Dong; Driehuis, Else; Sawyers, Charles L.; Chen, Yu; Clevers, Hans (2016): Organoid culture systems for prostate epithelial and cancer tissue. In *Nature protocols* 11 (2), pp. 347–358. DOI: 10.1038/nprot.2016.006.

Drost, Jarno; van Jaarsveld, Richard H.; Ponsioen, Bas; Zimberlin, Cheryl; van Boxtel, Ruben; Buijs, Arjan et al. (2015): Sequential cancer mutations in cultured human intestinal stem cells. In *Nature* 521 (7550), pp. 43–47. DOI: 10.1038/nature14415.

Eastham, J. A.; Hall, S. J.; Sehgal, I.; Wang, J.; Timme, T. L.; Yang, G. et al. (1995): In vivo gene therapy with p53 or p21 adenovirus for prostate cancer. In *Cancer research* 55 (22), pp. 5151–5155.

Ecke, Thorsten H.; Schlechte, Horst H.; Hübsch, Anne; Lenk, Severin V.; Schiemenz, Katrin; Rudolph, Birgit D.; Miller, Kurt (2007): TP53 mutation in prostate needle biopsies--comparison with patients follow-up. In *Anticancer research* 27 (6B), pp. 4143–4148.

Gao, Dong; Vela, Ian; Sboner, Andrea; Iaquinta, Phillip J.; Karthaus, Wouter R.; Gopalan, Anuradha et al. (2014): Organoid cultures derived from patients with advanced prostate cancer. In *Cell* 159 (1), pp. 176–187. DOI: 10.1016/j.cell.2014.08.016.

Gleason, Donald F.; Mellinger, George T. (1974): Prediction of Prognosis for Prostatic Adenocarcinoma by Combined Histological Grading and Clinical Staging. In *Journal of Urology* 111 (1), pp. 58–64. DOI: 10.1016/s0022-5347(17)59889-4.

Gorgoulis, Vassilis G.; Vassiliou, Leandros-Vassilios F.; Karakaidos, Panagiotis; Zacharatos, Panayotis; Kotsinas, Athanassios; Liloglou, Triantafillos et al. (2005): Activation of the DNA damage checkpoint and genomic instability in human precancerous lesions. In *Nature* 434 (7035), pp. 907–913. DOI: 10.1038/nature03485.

Grabowska, Magdalena M.; DeGraff, David J.; Yu, Xiuping; Jin, Ren Jie; Chen, Zhenbang; Borowsky, Alexander D.; Matusik, Robert J. (2014): Mouse models of prostate cancer: picking the best model

for the question. In *Cancer metastasis reviews* 33 (2-3), pp. 377–397. DOI: 10.1007/s10555-013-9487-8.

Guo, Caiying; Yang, Wenyi; Lobe, Corrinne G. (2002): A Cre recombinase transgene with mosaic, widespread tamoxifen-inducible action. In *Genesis (New York, N.Y. : 2000)* 32 (1), pp. 8–18. DOI: 10.1002/gene.10021.

Haffner, Michael C.; Mosbruger, Timothy; Esopi, David M.; Fedor, Helen; Heaphy, Christopher M.; Walker, David A. et al. (2013): Tracking the clonal origin of lethal prostate cancer. In *The Journal of clinical investigation* 123 (11), pp. 4918–4922. DOI: 10.1172/JCI70354.

Hill, Reginald; Song, Yurong; Cardiff, Robert D.; van Dyke, Terry (2005): Selective evolution of stromal mesenchyme with p53 loss in response to epithelial tumorigenesis. In *Cell* 123 (6), pp. 1001–1011. DOI: 10.1016/j.cell.2005.09.030.

Horinaga, Minoru; Okita, Hajime; Nakashima, Jun; Kanao, Kent; Sakamoto, Michiie; Murai, Masaru (2005): Clinical and pathologic significance of activation of signal transducer and activator of transcription 3 in prostate cancer. In *Urology* 66 (3), pp. 671–675. DOI: 10.1016/j.urology.2005.03.066.

Horoszewicz, J. S.; Leong, S. S.; Kawinski, E.; Karr, J. P.; Rosenthal, H.; Chu, T. M. et al. (1983): LNCaP model of human prostatic carcinoma. In *Cancer Res* 43 (4), pp. 1809–1818.

Hu, Qian; Peng, Jing; Liu, Weiping; He, Xiaoli; Cui, Ling; Chen, Xinlian et al. (2014): Elevated cleaved caspase-3 is associated with shortened overall survival in several cancer types. In *International journal of clinical and experimental pathology* 7 (8), pp. 5057–5070.

Huang, Qian; Li, Fang; Liu, Xinjian; Li, Wenrong; Shi, Wei; Liu, Fei-Fei et al. (2011): Caspase 3-mediated stimulation of tumor cell repopulation during cancer radiotherapy. In *Nature medicine* 17 (7), pp. 860–866. DOI: 10.1038/nm.2385.

Huch, Meritxell; Koo, Bon-Kyoung (2015): Modeling mouse and human development using organoid cultures. In *Development (Cambridge, England)* 142 (18), pp. 3113–3125. DOI: 10.1242/dev.118570.

Hudson, D. L. (2004): Epithelial stem cells in human prostate growth and disease. In *Prostate Cancer and Prostatic Diseases* 7 (3), pp. 188–194. DOI: 10.1038/sj.pcan.4500745.

Humphrey, Peter A. (2012): Histological variants of prostatic carcinoma and their significance. In *Histopathology* 60 (1), pp. 59–74. DOI: 10.1111/j.1365-2559.2011.04039.x.

Humphrey, Peter A.; Moch, Holger; Cubilla, Antonio L.; Ulbright, Thomas M.; Reuter, Victor E. (2016): The 2016 WHO Classification of Tumours of the Urinary System and Male Genital Organs-Part B: Prostate and Bladder Tumours. In *European urology* 70 (1), pp. 106–119. DOI: 10.1016/j.eururo.2016.02.028.

Irshad, Shazia; Abate-Shen, Cory (2013): Modeling prostate cancer in mice: something old, something new, something premalignant, something metastatic. In *Cancer metastasis reviews* 32 (1-2), pp. 109–122. DOI: 10.1007/s10555-012-9409-1.

J.E. McNeal (1983): The prostate gland: morphology and pathobiology, pp. 3–37.

Jacks, Tyler; Remington, Lee; Williams, Bart O.; Schmitt, Earlene M.; Halachmi, Schlomit; Bronson, Roderick T.; Weinberg, Robert A. (1994): Tumor spectrum analysis in p53-mutant mice. In *Current Biology* 4 (1), pp. 1–7. DOI: 10.1016/s0960-9822(00)00002-6.

Jackson, Stephen P.; Bartek, Jiri (2009): The DNA-damage response in human biology and disease. In *Nature* 461 (7267), pp. 1071–1078. DOI: 10.1038/nature08467.

Jain, Anil K.; Raina, Komal; Agarwal, Rajesh (2013): Deletion of p21/Cdkn1a confers protective effect against prostate tumorigenesis in transgenic adenocarcinoma of the mouse prostate model. In *Cell cycle (Georgetown, Tex.)* 12 (10), pp. 1598–1604. DOI: 10.4161/cc.24741.

Jamaspishvili, Tamara; Berman, David M.; Ross, Ashley E.; Scher, Howard I.; Marzo, Angelo M. de; Squire, Jeremy A.; Lotan, Tamara L. (2018): Clinical implications of PTEN loss in prostate cancer. In *Nature reviews. Urology* 15 (4), pp. 222–234. DOI: 10.1038/nrurol.2018.9.

Jenkins, Lisa M. Miller; Durell, Stewart R.; Mazur, Sharlyn J.; Appella, Ettore (2012): p53 N-terminal phosphorylation: a defining layer of complex regulation. In *Carcinogenesis* 33 (8), pp. 1441–1449. DOI: 10.1093/carcin/bgs145.

Johnson, Daniel E.; O'Keefe, Rachel A.; Grandis, Jennifer R. (2018): Targeting the IL-6/JAK/STAT3 signalling axis in cancer. In *Nature reviews. Clinical oncology* 15 (4), pp. 234–248. DOI: 10.1038/nrclinonc.2018.8.

Josson, Sajni; Matsuoka, Yasuhiro; Chung, Leland W. K.; Zhau, Haiyen E.; Wang, Ruoxiang (2010): Tumor-stroma co-evolution in prostate cancer progression and metastasis. In *Seminars in cell & developmental biology* 21 (1), pp. 26–32. DOI: 10.1016/j.semcdb.2009.11.016.

Kaighn, M. E.; Lechner, J. F.; Narayan, K. S.; Jones, L. W. (1978): Prostate carcinoma: tissue culture cell lines. In *National Cancer Institute monograph* (49), pp. 17–21.

Karthaus, Wouter R.; Iaquinta, Phillip J.; Drost, Jarno; Gracanin, Ana; van Boxtel, Ruben; Wongvipat, John et al. (2014): Identification of multipotent luminal progenitor cells in human prostate organoid cultures. In *Cell* 159 (1), pp. 163–175. DOI: 10.1016/j.cell.2014.08.017.

Kastan, Michael B.; Bartek, Jiri (2004): Cell-cycle checkpoints and cancer. In *Nature* 432 (7015), pp. 316–323. DOI: 10.1038/nature03097.

Kelman, Z.; Prokocimer, M.; Peller, S.; Kahn, Y.; Rechavi, G.; Manor, Y. et al. (1989): Rearrangements in the p53 gene in Philadelphia chromosome positive chronic myelogenous leukemia. In *Blood* 74 (7), pp. 2318–2324.

Kleinman, Hynda K.; Martin, George R. (2005): Matrigel: basement membrane matrix with biological activity. In *Seminars in cancer biology* 15 (5), pp. 378–386. DOI: 10.1016/j.semcancer.2005.05.004.

Klocker, H.; Culig, Z.; Kaspar, F.; Hobisch, A.; Eberle, J.; Reissigl, A.; Bartsch, G. (1994): Androgen signal transduction and prostatic carcinoma. In *World journal of urology* 12 (2), pp. 99–103. DOI: 10.1007/bf00184245.

Kovacs, Erika; Zorn, Julie Anne; Huang, Yongjian; Barros, Tiago; Kuriyan, John (2015): A structural perspective on the regulation of the epidermal growth factor receptor. In *Annual review of biochemistry* 84, pp. 739–764. DOI: 10.1146/annurev-biochem-060614-034402.

Kuo, Linda J.; Yang, Li-Xi (2008): Gamma-H2AX - a novel biomarker for DNA double-strand breaks. In *In vivo (Athens, Greece)* 22 (3), pp. 305–309.

Kusaba, T.; Nakayama, T.; Yamazumi, K.; Yakata, Y.; Yoshizaki, A.; Nagayasu, T.; Sekine, I. (2005): Expression of p-STAT3 in human colorectal adenocarcinoma and adenoma; correlation with clinicopathological factors. In *Journal of clinical pathology* 58 (8), pp. 833–838. DOI: 10.1136/jcp.2004.023416.

Lamm, M. L.; Podlasek, C. A.; Barnett, D. H.; Lee, J.; Clemens, J. Q.; Hebner, C. M.; Bushman, W. (2001): Mesenchymal factor bone morphogenetic protein 4 restricts ductal budding and branching morphogenesis in the developing prostate. In *Developmental Biology* 232 (2), pp. 301–314. DOI: 10.1006/dbio.2001.0187.

Lancaster, Madeline A.; Knoblich, Juergen A. (2014): Organogenesis in a dish: modeling development and disease using organoid technologies. In *Science (New York, N.Y.)* 345 (6194), p. 1247125. DOI: 10.1126/science.1247125.

Lapointe, Jacques; Li, Chunde; Giacomini, Craig P.; Salari, Keyan; Huang, Stephanie; Wang, Pei et al. (2007): Genomic profiling reveals alternative genetic pathways of prostate tumorigenesis. In *Cancer Res* 67 (18), pp. 8504–8510. DOI: 10.1158/0008-5472.CAN-07-0673.

Lesche, Ralf; Groszer, Matthias; Gao, Jing; Wang, Ying; Messing, Albee; Sun, Hong et al. (2002): Cre/loxP-mediated inactivation of the murine Pten tumor suppressor gene. In *Genesis (New York, N.Y. : 2000)* 32 (2), pp. 148–149. DOI: 10.1002/gene.10036.

Levy, David E.; Darnell, J. E. (2002): Stats: transcriptional control and biological impact. In *Nature reviews. Molecular cell biology* 3 (9), pp. 651–662. DOI: 10.1038/nrm909.

Li, M. L.; Aggeler, J.; Farson, D. A.; Hatier, C.; Hassell, J.; Bissell, M. J. (1987): Influence of a reconstituted basement membrane and its components on casein gene expression and secretion in mouse mammary epithelial cells. In *Proceedings of the National Academy of Sciences of the United States of America* 84 (1), pp. 136–140. DOI: 10.1073/pnas.84.1.136.

Li, Wen-Chang; Ye, Sheng-Long; Sun, Rui-Xia; Liu, Yin-Kun; Tang, Zhao-You; Kim, Youngsoo et al. (2006): Inhibition of growth and metastasis of human hepatocellular carcinoma by antisense oligonucleotide targeting signal transducer and activator of transcription 3. In *Clinical cancer research : an official journal of the American Association for Cancer Research* 12 (23), pp. 7140–7148. DOI: 10.1158/1078-0432.CCR-06-0484.

Liotta, L. A.; Kohn, E. C. (2001): The microenvironment of the tumour-host interface. In *Nature* 411 (6835), pp. 375–379. DOI: 10.1038/35077241.

Liu, Wennuan; Laitinen, Sari; Khan, Sofia; Vihinen, Mauno; Kowalski, Jeanne; Yu, Guoqiang et al. (2009): Copy number analysis indicates monoclonal origin of lethal metastatic prostate cancer. In *Nature medicine* 15 (5), pp. 559–565. DOI: 10.1038/nm.1944.

Liu, Xinjian; Li, Fang; Huang, Qian; Zhang, Zhengxiang; Zhou, Ling; Deng, Yu et al. (2017): Self-inflicted DNA double-strand breaks sustain tumorigenicity and stemness of cancer cells. In *Cell research* 27 (6), pp. 764–783. DOI: 10.1038/cr.2017.41.

Logothetis, Christopher J.; Lin, Sue-Hwa (2005): Osteoblasts in prostate cancer metastasis to bone. In *Nature reviews. Cancer* 5 (1), pp. 21–28. DOI: 10.1038/nrc1528.

Long, Michael A.; Rossi, Fabio M. V. (2009): Silencing inhibits Cre-mediated recombination of the Z/AP and Z/EG reporters in adult cells. In *PloS one* 4 (5), e5435. DOI: 10.1371/journal.pone.0005435.

Lotan, Tamara L.; Wei, Wei; Ludkovski, Olga; Morais, Carlos L.; Guedes, Liana B.; Jamaspishvili, Tamara et al. (2016): Analytic validation of a clinical-grade PTEN immunohistochemistry assay in prostate cancer by comparison with PTEN FISH. In *Modern pathology : an official journal of the United States and Canadian Academy of Pathology, Inc* 29 (8), pp. 904–914. DOI: 10.1038/modpathol.2016.88.

Maehama, T.; Dixon, J. E. (1998): The tumor suppressor, PTEN/MMAC1, dephosphorylates the lipid second messenger, phosphatidylinositol 3,4,5-trisphosphate. In *The Journal of biological chemistry* 273 (22), pp. 13375–13378. DOI: 10.1074/jbc.273.22.13375.

Manning, Brendan D.; Cantley, Lewis C. (2007): AKT/PKB signaling: navigating downstream. In *Cell* 129 (7), pp. 1261–1274. DOI: 10.1016/j.cell.2007.06.009.

Marker, Paul C.; Donjacour, Annemarie A.; Dahiya, Rajvir; Cunha, Gerald R. (2003): Hormonal, cellular, and molecular control of prostatic development. In *Developmental Biology* 253 (2), pp. 165–174. DOI: 10.1016/S0012-1606(02)00031-3.

Matano, Mami; Date, Shoichi; Shimokawa, Mariko; Takano, Ai; Fujii, Masayuki; Ohta, Yuki et al. (2015): Modeling colorectal cancer using CRISPR-Cas9-mediated engineering of human intestinal organoids. In *Nature medicine* 21 (3), pp. 256–262. DOI: 10.1038/nm.3802.

McGrath, Shannon; Christidis, Daniel; Perera, Marlon; Hong, Sung Kyu; Manning, Todd; Vela, Ian; Lawrentschuk, Nathan (2016): Prostate cancer biomarkers: Are we hitting the mark? In *Prostate international* 4 (4), pp. 130–135. DOI: 10.1016/j.prnil.2016.07.002.

McNeal, J. E.; Redwine, E. A.; Freiha, F. S.; Stamey, T. A. (1988): Zonal distribution of prostatic adenocarcinoma. Correlation with histologic pattern and direction of spread. In *The American journal of surgical pathology* 12 (12), pp. 897–906. DOI: 10.1097/00000478-198812000-00001.

Montironi, Rodolfo; Mazzucchelli, Roberta; Lopez-Beltran, Antonio; Cheng, Liang; Scarpelli, Marina (2007): Mechanisms of disease: high-grade prostatic intraepithelial neoplasia and other proposed preneoplastic lesions in the prostate. In *Nature clinical practice. Urology* 4 (6), pp. 321–332. DOI: 10.1038/ncpuro0815.

Mora, Linda B.; Buettner, Ralf; Seigne, John; Diaz, Jose; Ahmad, Nazeel; Garcia, Roy et al. (2002): Constitutive activation of Stat3 in human prostate tumors and cell lines: direct inhibition of Stat3 signaling induces apoptosis of prostate cancer cells. In *Cancer Res* 62 (22), pp. 6659–6666.

Muñoz, E.; Gómez, F.; Paz, J. I.; Casado, I.; Silva, J. M.; Corcuera, M. T.; Alonso, M. J. (2003): Ki-67 immunolabeling in pre-malignant lesions and carcinoma of the prostate. Histological correlation and prognostic evaluation. In *European journal of histochemistry : EJH* 47 (2), pp. 123–128. DOI: 10.4081/816.

Nigro, J. M.; Baker, S. J.; Preisinger, A. C.; Jessup, J. M.; Hostetter, R.; Cleary, K. et al. (1989): Mutations in the p53 gene occur in diverse human tumour types. In *Nature* 342 (6250), pp. 705–708. DOI: 10.1038/342705a0.

NOGUCHI, MASANORI; STAMEY, THOMAS A.; NEAL, JOHN E.Mc; YEMOTO, CHERYL E.M. (2000): AN ANALYSIS OF 148 CONSECUTIVE TRANSITION ZONE CANCERS: CLINICAL AND HISTOLOGICAL CHARACTERISTICS. In *Journal of Urology* 163 (6), pp. 1751–1755. DOI: 10.1016/S0022-5347(05)67535-0.

Peehl, D. M. (2005): Primary cell cultures as models of prostate cancer development. In *Endocrine-related cancer* 12 (1), pp. 19–47. DOI: 10.1677/erc.1.00795.

Pencik, Jan; Schlederer, Michaela; Gruber, Wolfgang; Unger, Christine; Walker, Steven M.; Chalaris, Athena et al. (2015a): STAT3 regulated ARF expression suppresses prostate cancer metastasis. In *Nature communications* 6, p. 7736. DOI: 10.1038/ncomms8736.

Pencik, Jan; Wiebringhaus, Robert; Susani, Martin; Culig, Zoran; Kenner, Lukas (2015b): IL-6/STAT3/ARF: the guardians of senescence, cancer progression and metastasis in prostate cancer. In *Swiss medical weekly* 145, w14215. DOI: 10.4414/smw.2015.14215.

Purdie, C. A.; Harrison, D. J.; Peter, A.; Dobbie, L.; White, S.; Howie, S. E. et al. (1994): Tumour incidence, spectrum and ploidy in mice with a large deletion in the p53 gene. In *Oncogene* 9 (2), pp. 603–609.

Roy-Burman, P.; Wu, H.; Powell, W. C.; Hagenkord, J.; Cohen, M. B. (2004): Genetically defined mouse models that mimic natural aspects of human prostate cancer development. In *Endocrine-related cancer*, pp. 225–254. DOI: 10.1677/erc.0.0110225.

Sato, Toshiro; Stange, Daniel E.; Ferrante, Marc; Vries, Robert G. J.; van Es, Johan H.; van den Brink, Stieneke et al. (2011): Long-term expansion of epithelial organoids from human colon, adenoma, adenocarcinoma, and Barrett's epithelium. In *Gastroenterology* 141 (5), pp. 1762–1772. DOI: 10.1053/j.gastro.2011.07.050.

Schaper, Fred; Rose-John, Stefan (2015): Interleukin-6: Biology, signaling and strategies of blockade. In *Cytokine & growth factor reviews* 26 (5), pp. 475–487. DOI: 10.1016/j.cytogfr.2015.07.004.

Schlechte, H. H.; Schnorr, D.; Löning, T.; Rudolph, B. D.; Pohrt, U. M.; Loening, S. A. (1997): Mutation of the tumor suppressor gene p53 in human prostate and bladder cancers--investigation by temperature gradient gel electrophoresis (TGGE). In *Journal of Urology* 157 (3), pp. 1049–1053.

Schlessinger, J.; Schreiber, A. B.; Levi, A.; Lax, I.; Libermann, T.; Yarden, Y. (1983): Regulation of cell proliferation by epidermal growth factor. In *CRC critical reviews in biochemistry* 14 (2), pp. 93–111. DOI: 10.3109/10409238309102791.

Scholzen, T.; Gerdes, J. (2000): The Ki-67 protein: from the known and the unknown. In *Journal of cellular physiology* 182 (3), pp. 311–322. DOI: 10.1002/(SICI)1097-4652(200003)182:3<311::AID-JCP1>3.0.CO;2-9.

Schwank, Gerald; Koo, Bon-Kyoung; Sasselli, Valentina; Dekkers, Johanna F.; Heo, Inha; Demircan, Turan et al. (2013): Functional repair of CFTR by CRISPR/Cas9 in intestinal stem cell organoids of cystic fibrosis patients. In *Cell stem cell* 13 (6), pp. 653–658. DOI: 10.1016/j.stem.2013.11.002.

Shappell, Scott B.; Thomas, George V.; Roberts, Richard L.; Herbert, Ron; Ittmann, Michael M.; Rubin, Mark A. et al. (2004): Prostate Pathology of Genetically Engineered Mice: Definitions and Classification. The Consensus Report from the Bar Harbor Meeting of the Mouse Models of Human Cancer Consortium Prostate Pathology Committee. In *Cancer Res* 64 (6), pp. 2270–2305. DOI: 10.1158/0008-5472.CAN-03-0946.

Shen, Wen Hong; Balajee, Adayabalam S.; Wang, Jianli; Wu, Hong; Eng, Charis; Pandolfi, Pier Paolo; Yin, Yuxin (2007): Essential role for nuclear PTEN in maintaining chromosomal integrity. In *Cell* 128 (1), pp. 157–170. DOI: 10.1016/j.cell.2006.11.042.

Shiloh, Yosef (2003): ATM and related protein kinases: safeguarding genome integrity. In *Nature reviews. Cancer* 3 (3), pp. 155–168. DOI: 10.1038/nrc1011.

Silver, Debra L.; Naora, Honami; Liu, Jinsong; Cheng, Wenjun; Montell, Denise J. (2004): Activated signal transducer and activator of transcription (STAT) 3: localization in focal adhesions and function in ovarian cancer cell motility. In *Cancer Res* 64 (10), pp. 3550–3558. DOI: 10.1158/0008-5472.CAN-03-3959.

Song, Min Sup; Salmena, Leonardo; Pandolfi, Pier Paolo (2012): The functions and regulation of the PTEN tumour suppressor. In *Nature reviews. Molecular cell biology* 13 (5), pp. 283–296. DOI: 10.1038/nrm3330.

Stewart, Bernard W.; Wild, Chris (Eds.) (2014): World cancer report 2014. International Agency for Research on Cancer; World Health Organization. Lyon France, Geneva Switzerland: International Agency for Research on Cancer; WHO Press World Health Organization.

Stone, K. R.; Mickey, D. D.; Wunderli, H.; Mickey, G. H.; Paulson, D. F. (1978): Isolation of a human prostate carcinoma cell line (DU 145). In *International journal of cancer* 21 (3), pp. 274–281. DOI: 10.1002/ijc.2910210305.

Sugimura, Y.; Cunha, G. R.; Donjacour, A. A.; Bigsby, R. M.; Brody, J. R. (1986): Whole-mount autoradiography study of DNA synthetic activity during postnatal development and androgen-induced regeneration in the mouse prostate. In *Biology of reproduction* 34 (5), pp. 985–995. DOI: 10.1095/biolreprod34.5.985.

Takahashi, T.; Nau, M. M.; Chiba, I.; Birrer, M. J.; Rosenberg, R. K.; Vinocour, M. et al. (1989): p53: a frequent target for genetic abnormalities in lung cancer. In *Science (New York, N.Y.)* 246 (4929), pp. 491–494. DOI: 10.1126/science.2554494.

Taplin, M. E.; Ho, S. M. (2001): Clinical review 134: The endocrinology of prostate cancer. In *The Journal of clinical endocrinology and metabolism* 86 (8), pp. 3467–3477. DOI: 10.1210/jcem.86.8.7782.

Taylor, Barry S.; Schultz, Nikolaus; Hieronymus, Haley; Gopalan, Anuradha; Xiao, Yonghong; Carver, Brett S. et al. (2010): Integrative genomic profiling of human prostate cancer. In *Cancer Cell* 18 (1), pp. 11–22. DOI: 10.1016/j.ccr.2010.05.026.

The Molecular Taxonomy of Primary Prostate Cancer (2015). In *Cell* 163 (4), pp. 1011–1025.

Titford, M. (2005): The long history of hematoxylin. In *Biotechnic & histochemistry : official publication of the Biological Stain Commission* 80 (2), pp. 73–78. DOI: 10.1080/10520290500138372.

Tomlins, Scott A.; Rhodes, Daniel R.; Perner, Sven; Dhanasekaran, Saravana M.; Mehra, Rohit; Sun, Xiao-Wei et al. (2005): Recurrent fusion of TMPRSS2 and ETS transcription factor genes in prostate cancer. In *Science (New York, N.Y.)* 310 (5748), pp. 644–648. DOI: 10.1126/science.1117679.

Toso, Alberto; Revandkar, Ajinkya; Di Mitri, Diletta; Guccini, Ilaria; Proietti, Michele; Sarti, Manuela et al. (2014): Enhancing chemotherapy efficacy in Pten-deficient prostate tumors by activating the senescence-associated antitumor immunity. In *Cell reports* 9 (1), pp. 75–89. DOI: 10.1016/j.celrep.2014.08.044.

Trotman, Lloyd C.; Niki, Masaru; Dotan, Zohar A.; Koutcher, Jason A.; Di Cristofano, Antonio; Xiao, Andrew et al. (2003): Pten dose dictates cancer progression in the prostate. In *PLoS biology* 1 (3), E59. DOI: 10.1371/journal.pbio.0000059.

Tsai, Susan; McOlash, Laura; Palen, Katie; Johnson, Bryon; Duris, Christine; Yang, Qiuhui et al. (2018): Development of primary human pancreatic cancer organoids, matched stromal and immune cells and 3D tumor microenvironment models. In *BMC cancer* 18 (1), p. 335. DOI: 10.1186/s12885-018-4238-4.

Tuxhorn, J. A.; Ayala, G. E.; Rowley, D. R. (2001): Reactive stroma in prostate cancer progression. In *The Journal of urology* 166 (6), pp. 2472–2483.

van Leenders, Geert J.L.H.; Schalken, Jack A. (2003): Epithelial cell differentiation in the human prostate epithelium: Implications for the pathogenesis and therapy of prostate cancer. In *Critical Reviews in Oncology/Hematology* 46, pp. 3–10. DOI: 10.1016/S1040-8428(03)00059-3.

Vermeulen, Katrien; van Bockstaele, Dirk R.; Berneman, Zwi N. (2003): The cell cycle: a review of regulation, deregulation and therapeutic targets in cancer. In *Cell proliferation* 36 (3), pp. 131–149. DOI: 10.1046/j.1365-2184.2003.00266.x.

Vivanco, Igor; Sawyers, Charles L. (2002): The phosphatidylinositol 3-Kinase AKT pathway in human cancer. In *Nature reviews. Cancer* 2 (7), pp. 489–501. DOI: 10.1038/nrc839.

Vogan, K.; Bernstein, M.; Leclerc, J. M.; Brisson, L.; Brossard, J.; Brodeur, G. M. et al. (1993): Absence of p53 gene mutations in primary neuroblastomas. In *Cancer Res* 53 (21), pp. 5269–5273.

Vousden, Karen H.; Prives, Carol (2009): Blinded by the Light: The Growing Complexity of p53. In *Cell* 137 (3), pp. 413–431. DOI: 10.1016/j.cell.2009.04.037.

Wade Harper, J. (1993): The p21 Cdk-interacting protein Cip1 is a potent inhibitor of G1 cyclin-dependent kinases. In *Cell* 75 (4), pp. 805–816. DOI: 10.1016/0092-8674(93)90499-G.

Wang, Shunyou; Gao, Jing; Lei, Qunying; Rozengurt, Nora; Pritchard, Colin; Jiao, Jing et al. (2003): Prostate-specific deletion of the murine Pten tumor suppressor gene leads to metastatic prostate cancer. In *Cancer Cell* 4 (3), pp. 209–221. DOI: 10.1016/S1535-6108(03)00215-0.

Wang, Y. Z.; Wong, Y. C. (1997): Oncogenes and tumor suppressor genes in prostate cancer: a review. In *Urologic Oncology: Seminars and Original Investigations* 3 (2), pp. 41–46. DOI: 10.1016/S1078-1439(97)00021-5.

Weinstein, Michael H.; Signoretti, Sabina; Loda, Massimo (2002): Diagnostic utility of immunohistochemical staining for p63, a sensitive marker of prostatic basal cells. In *Modern pathology : an official journal of the United States and Canadian Academy of Pathology, Inc* 15 (12), pp. 1302–1308. DOI: 10.1097/01.MP.0000038460.95912.6E.

Weiss, P.; Taylor, A. C. (1960): RECONSTITUTION OF COMPLETE ORGANS FROM SINGLE-CELL SUSPENSIONS OF CHICK EMBRYOS IN ADVANCED STAGES OF DIFFERENTIATION. In *Proceedings of the National Academy of Sciences of the United States of America* 46 (9), pp. 1177–1185. DOI: 10.1073/pnas.46.9.1177.

Wilson, H. V. (1907): A NEW METHOD BY WHICH SPONGES MAY BE ARTIFICIALLY REARED. In *Science (New York, N.Y.)* 25 (649), pp. 912–915. DOI: 10.1126/science.25.649.912.

Wu, Xiantuo; Wu, Jian; Huang, Jiapeng; Powell, William C.; Zhang, JianFeng; Matusik, Robert J. et al. (2001): Generation of a prostate epithelial cell-specific Cre transgenic mouse model for tissue-specific gene ablation. In *Mechanisms of Development* 101 (1-2), pp. 61–69. DOI: 10.1016/s0925-4773(00)00551-7.

Wu, Xinyu; Gong, Shiaoching; Roy-Burman, Pradip; Lee, Peng; Culig, Zoran (2013): Current mouse and cell models in prostate cancer research. In *Endocrine-related cancer* 20 (4), R155-70. DOI: 10.1530/ERC-12-0285.

Xu, Hanxiao; Lyu, Xiaodong; Yi, Ming; Zhao, Weiheng; Song, Yongping; Wu, Kongming (2018): Organoid technology and applications in cancer research. In *Journal of hematology & oncology* 11 (1), p. 116. DOI: 10.1186/s13045-018-0662-9.

Yoshimoto, M.; Cunha, I. W.; Coudry, R. A.; Fonseca, F. P.; Torres, C. H.; Soares, F. A.; Squire, J. A. (2007): FISH analysis of 107 prostate cancers shows that PTEN genomic deletion is associated with poor clinical outcome. In *British journal of cancer* 97 (5), pp. 678–685. DOI: 10.1038/sj.bjc.6603924.

Yoshimoto, Maisa; Cutz, Jean-Claude; Nuin, Paulo A. S.; Joshua, Anthony M.; Bayani, Jane; Evans, Andrew J. et al. (2006): Interphase FISH analysis of PTEN in histologic sections shows genomic deletions in 68% of primary prostate cancer and 23% of high-grade prostatic intra-epithelial neoplasias. In *Cancer genetics and cytogenetics* 169 (2), pp. 128–137. DOI: 10.1016/j.cancergencyto.2006.04.003.

Zhang, Dingxiao; Zhao, Shuhong; Li, Xinyun; Kirk, Jason S.; Tang, Dean G. (2018): Prostate Luminal Progenitor Cells in Development and Cancer. In *Trends in cancer* 4 (11), pp. 769–783. DOI: 10.1016/j.trecan.2018.09.003.

Zhang, Siyuan; Huang, Wen-Chien; Li, Ping; Guo, Hua; Poh, Say-Bee; Brady, Samuel W. et al. (2011): Combating trastuzumab resistance by targeting SRC, a common node downstream of multiple resistance pathways. In *Nature medicine* 17 (4), pp. 461–469. DOI: 10.1038/nm.2309.

Abstract

Cancer represents a major today's health problem and is responsible for many deaths globally each year with prostate cancer being the most diagnosed cancer in men in over half of the countries worldwide. The research invested in studying cancer and its properties has been on the rise in the last decades in order to uncover its causes, pathologies and to develop new treatments. Even though the prevalence of prostate cancer is relatively high, the lack of suitable *in vitro* model systems has hindered the progress of prostate cancer research. While in the last decades, 2D cell culture systems and animal model systems have been the basis of prostate cancer studies, new possibilities and technologies have emerged over time. For instance, the novel organoid technology gained attention in recent years for its large applications in cancer research. While prostate organoids derived from human primary prostate cancer have proven to be challenging to maintain in culture over long period of time, murine primary prostate cancer organoids have been successfully established and account for an alternative *in vitro* model system to study human prostate cancer.

In order to exploit this novel model system, we established a panel of murine benign and malignant prostate epithelial organoids, harbouring different genetic knockouts of prostate cancer relevant genes such as a single knockout of *Pten* and double knockouts of *Pten/Stat3* and *Pten/Tp53.* We characterized those organoid cultures with histological HE staining and various immunohistochemistry stainings such as Ki67, pAKT, STAT3 and CK8. We show that both benign and malignant organoids highly resemble their tissue of origin histologically and also regarding their signalling pathways. We also generated *in vitro* knockouts of *Pten* and *Pten/Stat3* genes from wildtype mice with floxed alleles using the Cre-lox recombination system *in vitro*. We demonstrate that deletion of both *Pten* and *Pten/Stat3* transform wildtype to malignant organoids over time and mimic the prostate cancer phenotypes that are seen *in vivo*. We propose this *in vitro* knockout system as a new model system to study tumorigenesis.

In conclusion, while human primary prostate cancer organoids have not been successfully established as long term cultures so far, we show that murine prostate organoids serve as a suitable alternative model system for prostate cancer. In the future we aim to establish

co-cultures containing also the immune and stromal components of the prostate tumour to further increase the accuracy of this model as a preclinical prostate cancer model.

Zusammenfassung

Krebs stellt heutzutage ein großes Gesundheitsproblem dar und ist jedes Jahr weltweit für viele Todesfälle verantwortlich. Prostatakrebs ist in mehr als der Hälfte der Länder weltweit der am häufigsten diagnostizierte Krebs bei Männern. Die Forschungsmittel, die in die Untersuchung von Krebs und seine Eigenschaften investiert worden sind, um die Ursachen und Pathologien aufzudecken und neue Therapien zu entwickeln, haben in den letzten Jahrzehnten zugenommen. Obwohl die Prävalenz von Prostatakrebs relativ hoch ist, hat das Fehlen geeigneter *In-vitro*-Modellsysteme den Fortschritt der Prostatakrebsforschung eingeschränkt. Während in den letzten Jahrzehnten 2D-Zellkultursysteme und Tiermodellsysteme die Grundlage für Prostatakrebsstudien waren, haben sich im Laufe der Zeit neue Möglichkeiten und Technologien herausgebildet. Beispielsweise hat die neuartige Organoidtechnologie in den letzten Jahren aufgrund ihrer großen Anwendungen in der Krebsforschung Aufmerksamkeit erregt. Bei Prostata-Organoiden, die aus dem primärem Prostatakrebs des Menschen stammen, hat es sich als schwierig erwiesen, über einen langen Zeitraum in der Kultur zu bleiben. Organoide des primären Prostatakrebses der Maus wurden jedoch erfolgreich etabliert und sind ein alternatives *In-vitro*-Modellsystem zur Untersuchung des menschlichen Prostatakrebses.

Um dieses neuartige Modellsystem zu nutzen, haben wir eine Gruppe von gutartigen und bösartigen Prostataepithelorganoiden der Maus eingerichtet, die verschiedene genetische Knockouts von Prostatakrebs-relevanten Genen enthalten, wie einen einzelnen Knockout von *Pten* und einen doppelten Knockout von P*ten*/*Stat3* und *Pten*/*Tp53*. Wir haben diese organoiden Kulturen mit histologischer HE-Färbung und verschiedenen immunhistochemischen Färbungen wie Ki67, pAKT, STAT3 und CK8 charakterisiert. Wir zeigen, dass sowohl gutartige als auch bösartige Organoide ihrem Ursprungsgewebe histologisch und auch hinsichtlich ihrer Signalwege stark ähneln. Wir haben auch *In-vitro*-Knockouts von *Pten*- und *Pten*/*Stat3*-Genen aus Wildtyp-Mäusen mit floxierten Allelen unter Verwendung des Cre-lox-Rekombinationssystems *in vitro* erzeugt. Wir zeigen, dass die Deletion von *Pten* und *Pten*/*Stat3* den Wildtyp im Laufe der Zeit in maligne Organoide umwandelt und die *in vivo* beobachteten Prostatakrebs-Phänotypen nachahmt. Wir schlagen dieses *In-vitro*-Knockout-System als neues Modellsystem zur Untersuchung der Tumorentstehung vor.

Zusammenfassend lässt sich sagen, dass humane primäre Prostatakrebs-Organoide bisher nicht erfolgreich als Langzeitkulturen etabliert worden sind. Wir zeigen jedoch, dass murine Prostata-Organoide als geeignetes alternatives Modellsystem für Prostatakrebs dienen. In der Zukunft wollen wir Co-Kulturen etablieren, die auch die Immun- und Stromakomponenten des Prostatatumors enthalten, um die Genauigkeit dieses Modells als präklinisches Prostatakrebsmodell weiter zu erhöhen.